Prepared for submission to JHEP

Radiative corrections to the $\tau^- \to (P_1P_2)^-\nu_\tau$ ($P_{1,2} = \pi, K$) decays

Rafel Escribano,[a,b] **Jesús Alejandro Miranda,**[b] **and Pablo Roig**[c]

[a] *Grup de Física Teòrica, Departament de Física, Universitat Autònoma de Barcelona, 08193 Bellaterra (Barcelona), Spain.*

[b] *Institut de Física d'Altes Energies (IFAE) and The Barcelona Institute of Science and Technology, Campus UAB, 08193 Bellaterra (Barcelona), Spain.*

[c] *Departamento de Física, Centro de Investigación y de Estudios Avanzados del Instituto Politécnico Nacional, Apdo. Postal 14-740, 07000 Ciudad de México, México.*

E-mail: rescriba@ifae.es, jmiranda@ifae.es, proig@fis.cinvestav.mx

Abstract: The radiative corrections to the $\tau^- \to (P_1P_2)^-\nu_\tau$ ($P_{1,2} = \pi, K$) decays are calculated for the first time. The structure-dependent contributions are obtained using Resonance Chiral Theory. Our results, whose uncertainty is dominated by the model-independent corrections, enable precise tests of CKM unitarity, lepton flavor universality, and non-standard interactions.

Contents

1 Introduction

Semileptonic tau decays are well-known to be a clean laboratory for studying QCD hadronisation at energies below ~ 1.8 GeV [1, 2], where the light-flavoured resonances play a key role. All non-perturbative information of the one-meson tau decays is encoded in the corresponding P decay constants, that are best determined in lattice QCD [3]. Two-meson tau decays are specified in terms of two form factors, whose knowledge has improved over the years thanks to the use of dispersion relations [4–16], and nourished with high quality measurements [17–24]. A similar good understanding of hadronization has not yet been achieved in three-meson tau decays [8, 25–33] or higher-multiplicity modes, preventing for the moment their use in searches for new physics.

On the contrary, one- and two-meson tau decays have enabled significant and promising new physics tests in recent years [34–46]. At the precision attained, radiative corrections for these decay modes become necessary, which motivated their improved evaluation for the $\tau^- \to P^- \nu_\tau$ case [43, 44, 47–49]. For the di-pion tau decays, the need for these corrections first stemmed from their use in the dispersive integral rendering the leading order hadronic vacuum polarization contribution to the muon $g-2$ [50–52], which was again the target of our recent analysis [53] (see also Refs. [54, 55]). Ref. [11] put forward that, assuming lepton universality, semileptonic kaon decay measurements could be used to predict the corresponding (crossing-symmetric) tau decays yielding a V_{us} determination closer to unitarity than with the tau decay branching ratios. In that work, the model-independent radiative corrections were taken into account and the structure-dependent ones were estimated (see also Ref. [56]), resulting in a relative large (conservative) uncertainty. Including these model-dependent effects is one of our main motivations. Instead of relying on lepton universality and checking CKM unitarity [11], one can in principle test the latter, comparing the crossed channels, or directly bind new physics non-standard interactions from $\tau^- \to (K\pi)^-\nu_\tau$ decays [38]. For completeness, we also include the radiative corrections to the di-kaon tau decays and recall our reference results for the di-pion mode [53]. As noted in Ref. [46], see Fig. 1 for instance, bounds on non-standard interactions from hadronic tau decays are competitive and complementary to those coming from LHC searches and electroweak precision observables. As a relevant example, the precise comparison of $\tau \to \pi^-\pi^0\nu_\tau(\gamma)$ to $e^+e^- \to \pi^+\pi^-(\gamma)$ data, which requires the radiative corrections computed in this work (see also Ref. [53]), are able to reduce the allowed new physics area (in the relevant Wilson coefficients plane) by a factor ~ 3 [46]. Real radiation was computed for the $\tau^- \to \eta^{(\prime)}\pi^-\nu_\tau$ decay channels in Ref. [57], showing that it can compete with the non-photon decays, as G-parity and electromagnetic suppressions compete. Finally, we also estimate the corresponding results for the $K^-\eta^{(\prime)}$ channels.

The structure of the paper is as follows. In section 2, we recall the model-independent description of the $\tau^- \to P_1^- P_2^0 \nu_\tau\gamma$ decays and give the leading model-dependent corrections for the $K\pi$, $K\bar{K}$ and $\pi\pi$ cases, where only the latter are known (see e.g. refs. [51, 53]). Branching ratios and spectra for the radiative decays are analyzed in section 3, and the corresponding radiative correction factors are computed in section 4. Finally, we conclude in section 5. Appendices cover $K_{\ell 3}$ decays (A), virtual corrections to di-meson tau decays (B), the non-radiative decays (C), and the kinematics of these three- and four-body processes (D).

2 The $\tau^- \to P_1^- P_2^0 \nu_\tau\gamma$ decays

The most general structure for these decays ($\tau(P) \to P_1^-(p_-)P_2^0(p_0)\nu_\tau(q)\gamma(k)$ is our momenta convention) is given by

$$\begin{aligned}\mathcal{M} =& \frac{eG_F V_{ud}^*}{\sqrt{2}}\epsilon_\mu^*\left[\frac{H_\nu(p_-,p_0)}{k^2-2k\cdot P}\bar{u}(q)\gamma^\nu(1-\gamma^5)(m_\tau+\not{P}-\not{k})\gamma^\mu u(P)\right.\\ &\left.+(V^{\mu\nu}-A^{\mu\nu})\bar{u}(q)\gamma_\nu(1-\gamma^5)u(P)\right] ,\end{aligned} \tag{2.1}$$

where the hadronic matrix element can be written as

$$H^\nu(p_-,p_0) = C_V F_+(t)Q^\nu + C_S\frac{\Delta_{-0}}{t}q^\nu F_0(t) , \tag{2.2}$$

with $t=q^2$, $Q^\nu = (p_- - p_0)^\nu - \frac{\Delta_{-0}}{t}q^\nu$, $q^\nu = (p_-+p_0)^\nu$, and $\Delta_{ij} = m_i^2 - m_j^2$. One recovers the usual definition of $H^\nu_{K\pi}$ [38] by replacing $p_- \to p_K$, $p_0 \to p_\pi$ and $\Delta_{-0} \to \Delta_{K\pi}$ for $K^-\pi^0$,

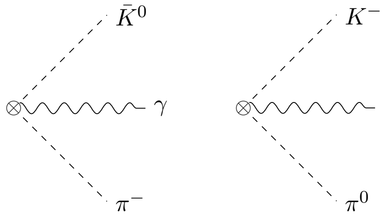

Figure 1. Feynman diagrams contributing to the term proportional to the metric tensor $g^{\mu\nu}$ in Eqs. (2.3) and (2.4).

and $p_- \to p_\pi$, $p_0 \to p_K$, $C_{V,S} \to -C_{V,S}$ and $\Delta_{-0} \to -\Delta_{K\pi}$ for $\bar{K}^0\pi^-$ (we comment on the identifications for the $P_1 = P_2$ channels below Fig. (1)). In all cases, gauge invariance implies $k_\mu V^{\mu\nu} = H^\nu(p_-, p_0)$ and $k_\mu A^{\mu\nu} = 0$.

The structure-independent term is given by

$$\begin{aligned}
V_{\rm SI}^{\mu\nu} =& \frac{H^\nu(p_K+k, p_\pi)(2p_K+k)^\mu}{2k\cdot p_K + k^2} + \left\{ -C_V F_+(t') - \frac{\Delta_{K\pi}}{t'}\left[C_S F_0(t') - C_V F_+(t')\right]\right\} g^{\mu\nu} \\
&- C_V \frac{F_+(t') - F_+(t)}{k\cdot(p_K+p_\pi)} Q^\nu q^\mu + \frac{\Delta_{K\pi}}{tt'} \left\{ 2\left[C_S F_0(t') - C_V F_+(t')\right] \right. \\
&\left. - \frac{C_S t'}{k\cdot(p_K+p_\pi)}\left[F_0(t') - F_0(t)\right]\right\} q^\mu q^\nu \ ,
\end{aligned} \tag{2.3}$$

where $C_V^{K^-\pi^0} = C_S^{K^-\pi^0} = 1/\sqrt{2}$ for $\tau^- \to K^-\pi^0\nu_\tau\gamma$, and

$$\begin{aligned}
V_{\rm SI}^{\mu\nu} =& \frac{H^\nu(p_K, p_\pi+k)(2p_\pi+k)^\mu}{2k\cdot p_\pi + k^2} + \left\{ C_V F_+(t') - \frac{\Delta_{K\pi}}{t'}\left[C_S F_0(t') - C_V F_+(t')\right]\right\} g^{\mu\nu} \\
&- C_V \frac{F_+(t') - F_+(t)}{k\cdot(p_K+p_\pi)} Q^\nu q^\mu + \frac{\Delta_{K\pi}}{tt'} \left\{ 2\left[C_S F_0(t') - C_V F_+(t')\right] \right. \\
&\left. - \frac{C_S t'}{k\cdot(p_K+p_\pi)}\left[F_0(t') - F_0(t)\right]\right\} q^\mu q^\nu \ ,
\end{aligned} \tag{2.4}$$

with $C_V^{\bar{K}^0\pi^-} = C_S^{\bar{K}^0\pi^-} = 1$ for $\tau^- \to \bar{K}^0\pi^-\nu_\tau\gamma$, and $t' = (P-q)^2$. The main difference between these two expressions comes from the sign in the term proportional to $g_{\mu\nu}$, which at leading order (LO) in Chiral Perturbation Theory (ChPT) is contributed by the diagrams in Fig. 1.

Conversely, $V_{\rm SI}^{\mu\nu}$ for the other tau decay modes can be obtained from Eq. (2.3) by substituting $p_K \to p_-$, $p_\pi \to p_0$ and $\Delta_{K\pi} \to \Delta_{-0}$. In particular, we are interested in the $\tau^- \to K^-K^0\nu_\tau\gamma$ decays where $C_V^{K^-K^0} = C_S^{K^-K^0} = -1$ [1].

[1] We comment briefly on the $P = \pi$ case at the end of Sec. 2.1, see Ref. [53].

The structure-dependent part is given by

$$V_{\rm SD}^{\mu\nu} = v_1(k\cdot p_- g^{\mu\nu} - k^\nu p_-^\mu) + v_2(k\cdot p_0 g^{\mu\nu} - k^\nu p_0^\mu) \\ + v_3(k\cdot p_0 p_-^\mu - k\cdot p_- p_0^\mu)p_-^\nu + v_4(k\cdot p_0 p_-^\mu - k\cdot p_- p_0^\mu)(p_- + p_0 + k)^\nu \ , \tag{2.5}$$

and

$$A_{\mu\nu} = ia_1 \epsilon_{\mu\nu\rho\sigma}\left(p_0 - p_-\right)^\rho k^\sigma + ia_2\left(P-q\right)_\nu \epsilon_{\mu\rho\sigma\tau} k^\rho p_-^\sigma p_0^\tau \\ + ia_3 \epsilon_{\mu\nu\rho\sigma} k^\rho (P-q)^\sigma + ia_4 (p_0+k)_\nu \epsilon_{\mu\lambda\rho\sigma} k^\lambda p_-^\rho p_0^\sigma \ , \tag{2.6}$$

where p_- and p_0 refer to the momentum of the charged and neutral meson, respectively.

From the last expressions, it is easy to show that the Low's theorem [58] is manifestly satisfied,

$$V^{\mu\nu} = \frac{p_-^\mu}{k\cdot p_-} H^\nu(p_-, p_0) + \left\{ C_V F_+(t) + \frac{\Delta_{-0}}{t}\left[C_S F_0(t) - C_V F_+(t)\right]\right\}\left(\frac{p_-^\mu k^\nu}{k\cdot p_-} - g^{\mu\nu}\right) \\ - \frac{2\Delta_{-0}}{t^2}\left[C_S F_0(t) - C_V F_+(t)\right]\left(\frac{k\cdot p_0}{k\cdot p_-} p_-^\mu - p_0^\mu\right)(p_- + p_0)^\nu \\ + 2\left(\frac{k\cdot p_0}{k\cdot p_-} p_-^\mu - p_0^\mu\right)\left[C_V \frac{dF_+(t)}{dt} Q^\nu + C_S \frac{\Delta_{-0}}{t} q^\nu \frac{dF_0(t)}{dt}\right] + \mathcal{O}(k) \ , \tag{2.7}$$

and the amplitude reads

$$\mathcal{M} = \frac{eG_F V_{uD}\sqrt{S_{\rm EW}}}{\sqrt{2}} \epsilon_\mu^*(k) H_\nu(p_-, p_0) \bar{u}(q)\gamma^\nu(1-\gamma^5)u(P) \\ \times \left(\frac{p_-^\mu}{k\cdot p_- + \frac{1}{2}M_\gamma^2} - \frac{P^\mu}{k\cdot P - \frac{1}{2}M_\gamma^2}\right) + \mathcal{O}(k^0) \ , \tag{2.8}$$

where $S_{\rm EW}$ encodes the short-distance electroweak corrections [59–66] and V_{uD} $(D = d, s)$ is the corresponding CKM matrix element.

In this limit, one gets

$$\overline{|\mathcal{M}|^2} = 2e^2 G_F^2 \left|V_{uD}\right|^2 S_{\rm EW}\left\{C_S^2 \left|F_0(t)\right|^2 D_0^{P^-P^0}(t,u) + C_S C_V {\rm Re}\left[F_+(t)F_0^*(t)\right] D_{+0}^{P^-P^0}(t,u) \right. \\ \left. + C_V^2 \left|F_+(t)\right|^2 D_+^{P^-P^0}(t,u)\right\} \sum_{\gamma\,\rm pols.}\left|\frac{p_-\cdot\epsilon}{p_-\cdot k} - \frac{P\cdot\epsilon}{P\cdot k}\right|^2 + \mathcal{O}(k^0) \ , \tag{2.9}$$

where

$$D_+^{P^-P^0}(t,u) = \frac{m_\tau^2}{2}(m_\tau^2 - t) + 2m_0^2 m_-^2 - 2u(m_\tau^2 - t + m_0^2 + m_-^2) + 2u^2 \\ + \frac{\Delta_{-0}}{t} m_\tau^2 (2u + t - m_\tau^2 - 2m_0^2) + \frac{\Delta_{-0}^2}{t^2}\frac{m_\tau^2}{2}(m_\tau^2 - t) \ , \tag{2.10}$$

$$D_0^{P^-P^0}(t,u) = \frac{\Delta_{-0}^2 m_\tau^4}{2t^2}\left(1-\frac{t}{m_\tau^2}\right) \ , \tag{2.11}$$

$$D_{+0}^{P^-P^0}(t,u) = \frac{\Delta_{0-} m_\tau^2}{t}\left[2u+t-m_\tau^2-2m_0^2+\frac{\Delta_{-0}}{t}(m_\tau^2-t)\right] \ , \tag{2.12}$$

with $u=(P-p_-)^2$. In this way, besides the Low theorem, the Burnet-Kroll one [67] is also explicitly manifest.

Thus, after an integration over neutrino and photon 4-momenta, the differential decay width in this approximation reads

$$\begin{aligned}\left.\frac{d\Gamma^{(0)}}{dt\,du}\right|_{PP\gamma} =& \frac{G_F^2|V_{uD}|^2 S_{\rm EW}}{128\pi^3 m_\tau^3}\left\{C_S^2\,|F_0(t)|^2\,D_0^{P^-P^0}(t,u)+C_V C_S {\rm Re}\left[F_+^*(t)F_0(t)\right] D_{+0}^{P^-P^0}(t,u)\right.\\ &\left.+C_V^2\,|F_+(t)|^2\,D_+^{P^-P^0}(t,u)\right\} g_{\rm rad}(t,u,M_\gamma) \ ,\end{aligned} \tag{2.13}$$

where (see Refs. [50, 51])

$$g_{\rm rad}(t,u,M_\gamma) = g_{\rm brems}(t,u,M_\gamma)+g_{\rm rest}(t,u) \ , \tag{2.14}$$

with

$$g_{\rm brems}(t,u,M_\gamma) = \frac{\alpha}{\pi}\left(J_{11}(t,u,M_\gamma)+J_{20}(t,u,M_\gamma)+J_{02}(t,u,M_\gamma)\right) \ , \tag{2.15a}$$

$$g_{\rm rest}(t,u) = \frac{\alpha}{\pi}\left(K_{11}(t,u)+K_{20}(t,u)+K_{02}(t,u)\right) \ . \tag{2.15b}$$

The expressions for $J_{ij}(t,u,M_\gamma)$ and $K_{ij}(t,u)$, which correspond to an integration over $\mathcal{D}^{\rm III}$ and $\mathcal{D}^{\rm IV/III}$, respectively, can be found in Refs. [11, 51, 53] and in App. D.

Integrating upon the u variable in Eq. (2.13), one gets

$$\begin{aligned}\left.\frac{d\Gamma}{dt}\right|_{\rm III} =& \frac{G_F^2 S_{\rm EW}|V_{uD}|^2 m_\tau^3}{384\pi^3 t}\left\{\frac{1}{2t^2}\left(1-\frac{t}{m_\tau^2}\right)^2\lambda^{1/2}(t,m_-^2,m_0^2)\right.\\ &\times\left[C_V^2\,|F_+(t)|^2\left(1+\frac{2t}{m_\tau^2}\right)\lambda(t,m_-^2,m_0^2)\overline{\delta}_+(t)+3C_S^2\Delta_{-0}^2\,|F_0(t)|^2\,\overline{\delta}_0(t)\right]\\ &\left.+C_S C_V\frac{4}{\sqrt{t}}\overline{\delta}_{+0}(t)\right\} \ ,\end{aligned} \tag{2.16}$$

with

$$\overline{\delta}_0(t) = \frac{\int_{u^-(t)}^{u^+(t)} D_0^{P^-P^0}(t,u)\,g_{\rm brems}(t,u,M_\gamma)du}{\int_{u^-(t)}^{u^+(t)} D_0^{P^-P^0}(t,u)\,du} \ , \tag{2.17}$$

$$\overline{\delta}_+(t) = \frac{\int_{u^-(t)}^{u^+(t)} D_+^{P^-P^0}(t,u)\,g_{\rm brems}(t,u,M_\gamma)du}{\int_{u^-(t)}^{u^+(t)} D_+^{P^-P^0}(t,u)\,du} \ , \tag{2.18}$$

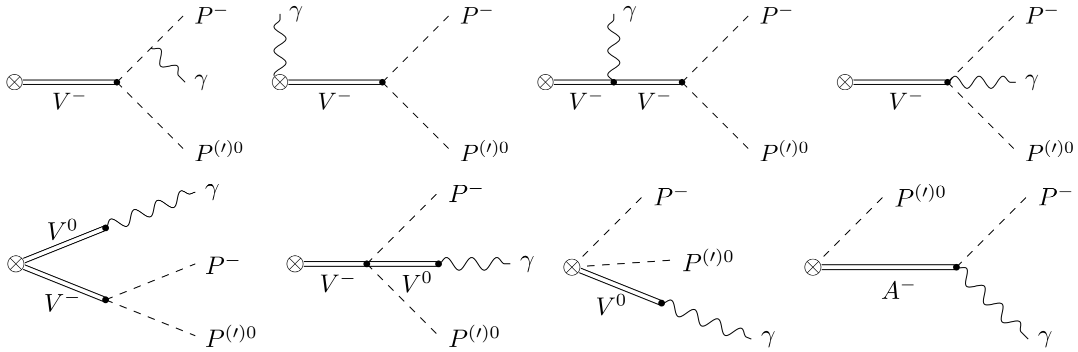

Figure 2. Vector and axial-vector meson exchange diagrams contributing to the $\tau^- \to P_1^- P_2^0 \nu_\tau \gamma$ decays at $\mathcal{O}\left(p^4\right)$. V^0 stands for the ρ^0, ω and ϕ resonances, $V^- = K^{*-}$ for the $K\pi$ modes and $V^- = \rho^-$ for the K^-K^0 one, and $A^- = K_1^-$ in K^-K^0 and $K^-\pi^0$, and $A^- = a_1^-$ in $\pi^-\bar{K}^0$.

$$\bar{\delta}_{+0}(t) = \frac{3t\sqrt{t}}{4m_\tau^6} \int_{u^-(t)}^{u^+(t)} D_{+0}^{P^-P^0}(t,u)\, g_{\text{brems}}(t,u,M_\gamma) \text{Re}\left[F_+^*(t) F_0(t)\right] du \,. \tag{2.19}$$

The remaining contribution, $d\Gamma/dt|_{\text{IV/III}}$, which corresponds to the integration over $\mathcal{D}_{\text{IV/III}}$ with $g_{\text{rest}}(t,u)$ instead of $g_{\text{brems}}(t,u,M_\gamma)$, is almost negligible and only becomes relevant near the threshold. In Ref. [68], the subleading contributions in the Low's approximation were studied, showing that they are not negligible and need to be taken into account to get a reliable estimation.

2.1 Vector contributions

Including those Lagrangian terms that, upon resonance integration, contribute to the ChPT $\mathcal{O}(p^4)$ low-energy constants (LECs) [2], we have found the following contributions to the vector form factors v_i in Eq. (2.5), which are depicted in Fig. 2:

$$\begin{aligned}
v_1 =& \frac{F_V G_V}{\sqrt{2} f^2 M_\rho^2} \left\{ \left(1 + \frac{1}{3}\frac{M_\rho^2}{M_\omega^2} + \frac{2}{3}\frac{M_\rho^2}{M_\phi^2}\right) \left[1 + \frac{1}{2}\left(t - \Delta_{K\pi}\right) D_{K^*}^{-1}(t)\right] \right.\\
&\left. + 2M_\rho^2 D_{K^*}^{-1}(t') + M_\rho^2 \left(t - \Delta_{K\pi}\right) D_{K^*}^{-1}(t) D_{K^*}^{-1}(t') \right\}\\
&+ \frac{F_V^2}{2\sqrt{2} f^2 M_\rho^2} \left[-\frac{1}{2}\left(1 + \frac{1}{3}\frac{M_\rho^2}{M_\omega^2} + \frac{2}{3}\frac{M_\rho^2}{M_\phi^2}\right)\left(1 - t'\, D_{K^*}^{-1}(t')\right) - M_\rho^2 D_{K^*}^{-1}(t') \right]\\
&+ \frac{F_A^2}{\sqrt{2} f^2 M_{K_1}^2} \left(M_{K_1}^2 - \frac{1}{2}\Sigma_{K\pi} + \frac{1}{2} t\right) D_{K_1}^{-1}[(p_K + k)^2] \,, \qquad (2.20a)\\
v_2 =& \frac{F_V G_V}{\sqrt{2} f^2 M_\rho^2} \left(t + \Delta_{K\pi}\right) \left[-\frac{1}{2}\left(1 + \frac{1}{3}\frac{M_\rho^2}{M_\omega^2} + \frac{2}{3}\frac{M_\rho^2}{M_\phi^2}\right) D_{K^*}^{-1}(t) - M_\rho^2 D_{K^*}^{-1}(t) D_{K^*}^{-1}(t') \right]
\end{aligned}$$

[2]We will simply write $\mathcal{O}(p^4)$ in the following to express that, although it is clear that for ChPT with resonances the chiral expansion is not applicable.

$$+\frac{F_V^2}{2\sqrt{2}f^2M_\rho^2}\left[-\frac{1}{2}\left(1+\frac{1}{3}\frac{M_\rho^2}{M_\omega^2}+\frac{2}{3}\frac{M_\rho^2}{M_\phi^2}\right)\left(1+t'\,D_{K^*}^{-1}(t')\right)-M_\rho^2D_{K^*}^{-1}(t')\right]$$

$$+\frac{F_A^2}{\sqrt{2}f^2M_{K_1}^2}\left(M_{K_1}^2-m_K^2-k\cdot p_K\right)D_{K_1}^{-1}[(p_K+k)^2]\ , \tag{2.20b}$$

$$v_3=\frac{F_A^2}{\sqrt{2}f^2M_{K_1}^2}D_{K_1}^{-1}[(p_K+k)^2]\ , \tag{2.20c}$$

$$v_4=-\frac{2F_VG_V}{\sqrt{2}f^2}D_{K^*}^{-1}(t)D_{K^*}^{-1}(t')+\frac{F_V^2}{2\sqrt{2}f^2M_\rho^2}\left(1+\frac{1}{3}\frac{M_\rho^2}{M_\omega^2}+\frac{2}{3}\frac{M_\rho^2}{M_\phi^2}\right)D_{K^*}^{-1}(t')\ , \tag{2.20d}$$

for $K^-\pi^0$,

$$v_1=-\frac{F_VG_V}{f^2M_\rho^2}\left[2+2M_\rho^2D_{K^*}^{-1}(t')+\frac{1}{2}\left(1+\frac{1}{3}\frac{M_\rho^2}{M_\omega^2}+\frac{2}{3}\frac{M_\rho^2}{M_\phi^2}\right)(t+\Delta_{K\pi})\,D_{K^*}^{-1}(t)\right.$$
$$\left.+(t+\Delta_{K\pi})\,M_\rho^2D_{K^*}^{-1}(t)D_{K^*}^{-1}(t')\right]$$
$$-\frac{F_V^2}{2f^2M_\rho^2}\left[-M_\rho^2D_{K^*}^{-1}(t')+\frac{1}{2}\left(1+\frac{1}{3}\frac{M_\rho^2}{M_\omega^2}+\frac{2}{3}\frac{M_\rho^2}{M_\phi^2}\right)t'\,D_{K^*}^{-1}(t')+\frac{1}{2}\left(-3+\frac{1}{3}\frac{M_\rho^2}{M_\omega^2}+\frac{2}{3}\frac{M_\rho^2}{M_\phi^2}\right)\right]$$
$$-\frac{F_A^2}{f^2M_{a_1}^2}\left(M_{a_1}^2-\frac{1}{2}\Sigma_{K\pi}+\frac{1}{2}t\right)D_{a_1}^{-1}[(p_\pi+k)^2]\ , \tag{2.21a}$$

$$v_2=-\frac{F_VG_V}{f^2M_\rho^2}\left\{(t-\Delta_{K\pi})\left[-M_\rho^2D_{K^*}^{-1}(t)D_{K^*}^{-1}(t')-\frac{1}{2}\left(1+\frac{1}{3}\frac{M_\rho^2}{M_\omega^2}+\frac{2}{3}\frac{M_\rho^2}{M_\phi^2}\right)D_{K^*}^{-1}(t)\right]\right.$$
$$\left.+1-\frac{1}{3}\frac{M_\rho^2}{M_\omega^2}-\frac{2}{3}\frac{M_\rho^2}{M_\phi^2}\right\}$$
$$-\frac{F_V^2}{2f^2M_\rho^2}\left[-M_\rho^2D_{K^*}^{-1}(t')-\frac{1}{2}\left(1+\frac{1}{3}\frac{M_\rho^2}{M_\omega^2}+\frac{2}{3}\frac{M_\rho^2}{M_\phi^2}\right)t'\,D_{K^*}^{-1}(t')+\frac{1}{2}\left(-3+\frac{1}{3}\frac{M_\rho^2}{M_\omega^2}+\frac{2}{3}\frac{M_\rho^2}{M_\phi^2}\right)\right]$$
$$-\frac{F_A^2}{f^2M_{a_1}^2}\left(M_{a_1}^2-m_\pi^2k\cdot p_\pi\right)D_{a_1}^{-1}[(p_\pi+k)^2]\ , \tag{2.21b}$$

$$v_3=-\frac{F_A^2}{f^2M_{a_1}^2}D_{a_1}^{-1}[(p_\pi+k)^2]\ , \tag{2.21c}$$

$$v_4=\frac{2F_VG_V}{f^2}D_{K^*}^{-1}(t)D_{K^*}^{-1}(t')-\frac{F_V^2}{2f^2M_\rho^2}\left(1+\frac{1}{3}\frac{M_\rho^2}{M_\omega^2}+\frac{2}{3}\frac{M_\rho^2}{M_\phi^2}\right)D_{K^*}^{-1}(t')\ , \tag{2.21d}$$

for $\bar{K}^0\pi^-$, and

$$v_1=-\frac{F_VG_V}{f^2M_\rho^2}\left[1+\frac{1}{3}\frac{M_\rho^2}{M_\omega^2}+\frac{2}{3}\frac{M_\rho^2}{M_\phi^2}+(t-\Delta_{K^-K^0})\,D_\rho^{-1}(t)+2M_\rho^2D_\rho^{-1}(t')\right.$$
$$\left.+M_\rho^2\,(t-\Delta_{K^-K^0})\,D_\rho^{-1}(t)D_\rho^{-1}(t')\right]$$

$$
\begin{aligned}
&- \frac{F_V^2}{2f^2 M_\rho^2}\left[-\frac{1}{3}\frac{M_\rho^2}{M_\omega^2} - \frac{2}{3}\frac{M_\rho^2}{M_\phi^2} + t'\, D_\rho^{-1}(t') - M_\rho^2 D_\rho^{-1}(t')\right] \\
&- \frac{F_A^2}{f^2 M_{K_1}^2}\left(M_{K_1}^2 - \frac{1}{2}\Sigma_{K^-K^0} + \frac{1}{2}t\right) D_{K_1}^{-1}[(p_- + k)^2]\ , \qquad (2.22a)\\
v_2 =& - \frac{F_V G_V}{f^2 M_\rho^2}\left[-1 + \frac{1}{3}\frac{M_\rho^2}{M_\omega^2} + \frac{2}{3}\frac{M_\rho^2}{M_\phi^2} - (t + \Delta_{K^-K^0})\, D_\rho^{-1}(t) - M_\rho^2\,(t + \Delta_{K^-K^0})\, D_\rho^{-1}(t) D_\rho^{-1}(t')\right] \\
&- \frac{F_V^2}{2f^2 M_\rho^2}\left[-\frac{1}{3}\frac{M_\rho^2}{M_\omega^2} - \frac{2}{3}\frac{M_\rho^2}{M_\phi^2} - t'\, D_\rho^{-1}(t') - M_\rho^2 D_\rho^{-1}(t')\right] \\
&- \frac{F_A^2}{f^2 M_{K_1}^2}\left(M_{K_1}^2 - m_{K^-}^2 - k\cdot p_-\right) D_{K_1}^{-1}[(p_- + k)^2]\ , \qquad (2.22b)\\
v_3 =& - \frac{F_A^2}{f^2 M_{K_1}^2} D_{K_1}^{-1}[(p_- + k)^2]\ , \qquad (2.22c)\\
v_4 =& \frac{2F_V G_V}{f^2} D_\rho^{-1}(t) D_\rho^{-1}(t') - \frac{F_V^2}{f^2 M_\rho^2} D_\rho^{-1}(t')\ , \qquad (2.22d)
\end{aligned}
$$

for K^-K^0, where $\Sigma_{-0} = m_-^2 + m_0^2$ and $D_R^{-1}(x) = M_R^2 - x - iM\Gamma_R(x)$. Off-shell resonance widths are given in terms of the leading pseudo-Goldstone boson cuts [26, 27, 69].

It is straightforward to show that, except for a Clebsch-Gordan coefficient (CGC) factor, one recovers the expressions found in Refs. [51, 53] for the vector form factors of the $\tau^- \to \pi^-\pi^0\nu_\tau\gamma$ decays, in the isospin-symmetry limit.

All the former resonance contributions are given in terms of three couplings: F_V, responsible for instance of the coupling of the vector resonance to the vector current; F_A for the couplings of the axial resonance; and G_V which yields, among others, vertices between the vector resonance and a couple of pseudo-Goldstone bosons (see e.g. Ref. [70] for more details).

2.2 Axial contributions

The Feynman diagrams that contribute to these decays are depicted in Figs. 3–5. At $\mathcal{O}(p^4)$, the axial form factors a_i in Eq. (2.6), which receive contributions from the Wess-Zumino-Witten functional [71, 72], are given by

$$
a_1 = \frac{N_c}{12\sqrt{2}\pi^2 f^2}\ , \quad a_2 = -\frac{N_c}{6\sqrt{2}\pi^2 f^2 (t' - m_K^2)}\ , \quad a_3 = -\frac{N_c}{24\sqrt{2}\pi^2 f^2}\ , \qquad (2.23)
$$

for $K^-\pi^0$,

$$
a_3 = -\frac{N_c}{24\pi^2 f^2}\ , \qquad (2.24)
$$

for $\bar{K}^0\pi^-$, and

$$
a_3 = \frac{N_c}{24\pi^2 f^2}\ , \qquad (2.25)
$$

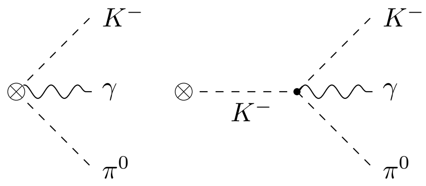

Figure 3. Axial contributions to the $\tau^- \to K^-\pi^0\nu_\tau\gamma$ decays at $\mathcal{O}\left(p^4\right)$.

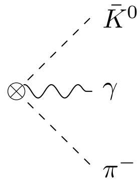

Figure 4. Axial contributions to the $\tau^- \to \bar{K}^0\pi^-\nu_\tau\gamma$ decays at $\mathcal{O}\left(p^4\right)$.

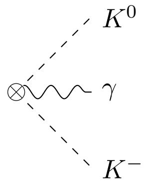

Figure 5. Axial contributions to the $\tau^- \to K^-K^0\nu_\tau\gamma$ decays at $\mathcal{O}\left(p^4\right)$.

for K^-K^0, where $N_c = 3$ is the number of colors and f is the pion decay constant in the chiral limit, $f \sim 90$ MeV.

In Fig. 5, only one diagram contributes to the $\tau^- \to K^-K^0\nu_\tau\gamma$ decays in a similar way to the $\tau^- \to \bar{K}^0\pi^-\nu_\tau\gamma$ decays. This is because the $K^- \to \bar{K}^0\pi^-\gamma$ (or $\pi^- \to K^-K^0\gamma$) vertex is absent in the WZW Lagrangian[3]. We reproduce the known anomalous contributions [51, 53] for the $\tau^- \to \pi^-\pi^0\nu_\tau\gamma$ case. We neglect resonance contributions in the anomalous sector, which start at $\mathcal{O}(p^6)$ in the chiral power counting [74].

3 Radiative hadronic tau decays

The differential rate for the $\tau^- \to P_1^- P_2^0\nu_\tau\gamma$ decays in the τ rest frame is given by

$$d\Gamma = \frac{(2\pi)^4}{4m_\tau}\sum_{\text{spin}}\overline{|\mathcal{M}|^2}d\Phi_4 \ , \tag{3.1}$$

[3]This feature was already studied for the $K_{\ell 3}$ decays in Ref. [73], where the non-local kaon pole term is only present in $A^+_{\mu\nu}$ for $K^+ \to \pi^0\ell^+\nu_\ell\gamma$ decays.

where $d\Phi_4$ is the corresponding 4-body phase space, given by

$$d\Phi_4 = \delta^{(4)}(P - p_- - p_0 - q - k)\frac{d^3p_-}{(2\pi)^3 2E_-}\frac{d^3p_0}{(2\pi)^3 2E_0}\frac{d^3q}{(2\pi)^3 2E_\nu}\frac{d^3k}{(2\pi)^3 2E_\gamma} \,, \tag{3.2}$$

and $\overline{|\mathcal{M}|^2}$ is the unpolarized spin-averaged squared amplitude. Inasmuch as this amplitude is not IR finite, we follow the same procedure as in Refs. [51, 53] where a photon energy cut, $E_\gamma^{\rm cut}$, was introduced to study the dynamics of the $\tau^- \to \pi^-\pi^0\nu_\tau\gamma$ decays.

In this analysis, we call "complete bremsstrahlung" or simply "SI" the amplitude with $v_{1,2,3,4} = a_{1,2,3,4} = 0$. For the $\mathcal{O}(p^4)$ contributions, as in Ref. [53], we distinguish between using the set of short-distance constraints $F_V = \sqrt{2}F$, $G_V = F/\sqrt{2}$ [75] and $F_A = F$; or $F_V = \sqrt{3}F$, $G_V = F/\sqrt{3}$ and $F_A = \sqrt{2}F$ [74, 76–78]. The former corresponds to the constraints from 2-point Green functions and the second to the values consistent up to 3-point Green functions which include operators that contribute at $\mathcal{O}(p^6)$ (that we are not including in this work). The difference between both sets of constraints has been employed to estimate roughly the model-dependent error of this approach [43, 44, 49, 53, 79]. In all our subsequent analyses, the $\mathcal{O}(p^4)$ results include the SI part and the structure dependent part (either with the $F_V = \sqrt{2}F$ or with the $F_V = \sqrt{3}F$ set of constraints).

Integrating Eq. (3.1) using the dispersive vector and scalar form factors [6, 7, 9, 13, 14, 80–82], we get the $P_1^- P_2^0$ invariant mass distribution, the photon energy distribution and the branching fraction as a function of $E_\gamma^{\rm cut}$. The outcomes are depicted in Figs. 6, 7, 8 and 9, and summarized in Tables 1, 2 and 3.

The branching fractions of the radiative decays as a function of $E_\gamma^{\rm cut}$ are shown in Fig. 6. In Tables 1 and 2, we can see that for $E_\gamma^{\rm cut} \lesssim 100\,\mathrm{MeV}$ the main contribution at $\mathcal{O}(p^4)$ comes from the complete bremsstrahlung (SI) amplitude in agreement with the results in Refs. [51, 53, 55] for the $\tau^- \to \pi^-\pi^0\nu_\tau\gamma$ decays. On the other hand, the Low's approximation is not sufficient to describe these decays for energies above 100 MeV. Contrary to the $\tau^- \to (K\pi)^-\nu_\tau$ transitions, where the $K^-\pi^0$ and $\pi^-\bar{K}^0$ decay modes differ only by a squared CGC factor, the radiative decays are more subtle. At low energies these two modes are approximately related by $\mathrm{Br}(\tau \to \bar{K}^0\pi^-\nu_\tau\gamma)/\mathrm{Br}(\tau^- \to K^-\pi^0\nu_\tau\gamma) \approx 2(m_K/m_\pi) \sim 7$, which explains their hierarchy (particularly, the relative size of the structure dependent —which basically scale according to the CGCs of the two decay channels— and the IB contributions), as seen in the following phenomenological analysis. Conversely, the $\tau^- \to K^-K^0\nu_\tau\gamma$ decays are more susceptible to SD contributions (see Table 3).

In Fig. 7, the decay spectrum is depicted with $v_i = a_i = 0$ for different $E_\gamma^{\rm cut}$ values. For the $\tau^- \to (K\pi)^-\nu_\tau\gamma$ decays, the first peak is due to bremsstrahlung off the charged meson i.e. K^- or π^-, and the second one receives contributions from bremsstrahlung off the τ lepton and resonance exchange.

In Fig. 8, we compare the distributions for $E_\gamma^{\rm cut} = 300\,\mathrm{MeV}$ using the Low's approximation (red dashed line), the SI amplitude (dotted line), and the $\mathcal{O}(p^4)$ amplitude with $F_V = \sqrt{2}F$ (dashed line) and $F_V = \sqrt{3}F$ (solid line). The most important contribution for the $(K\pi)^-$ decay channels comes from the $K^*(892)$ resonance exchange around $s \sim 0.79\,\mathrm{GeV}^2$. It is worth noting that for the $\tau^- \to \bar{K}^0\pi^-\nu_\tau\gamma$ decays there is a huge sup-

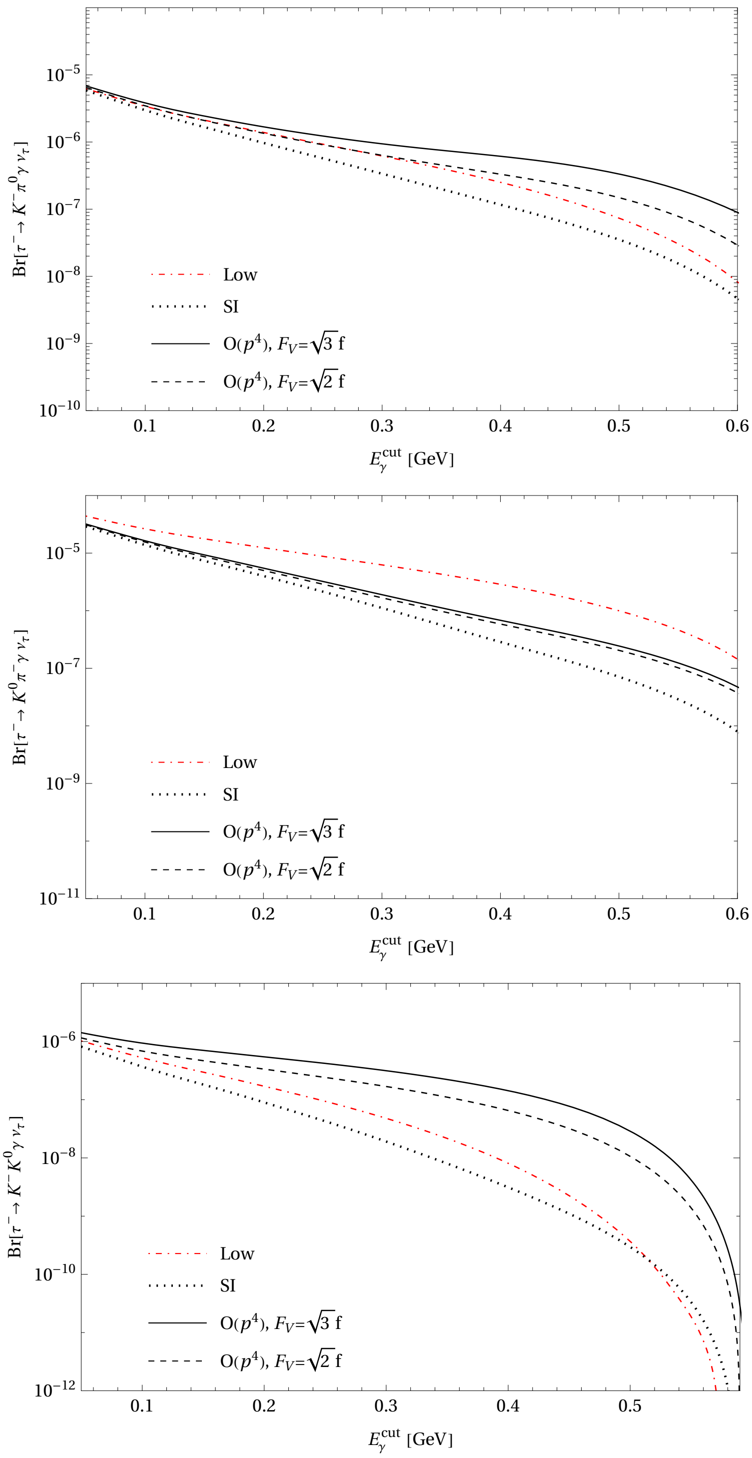

Figure 6. Branching ratio for the $\tau^- \to K^-\pi^0\nu_\tau\gamma$ (top), the $\tau^- \to \bar{K}^0\pi^-\nu_\tau\gamma$ (center) and the $\tau^- \to K^-K^0\nu_\tau\gamma$ (bottom) decays as a function of $E_\gamma^{\rm cut}$. The dotted line represents the bremsstrahlung contribution, the solid line and dashed line represent the $\mathcal{O}\left(p^4\right)$ corrections using $F_V = \sqrt{3}F$ and $F_V = \sqrt{2}F$, respectively. The red one corresponds to the Low approximation.

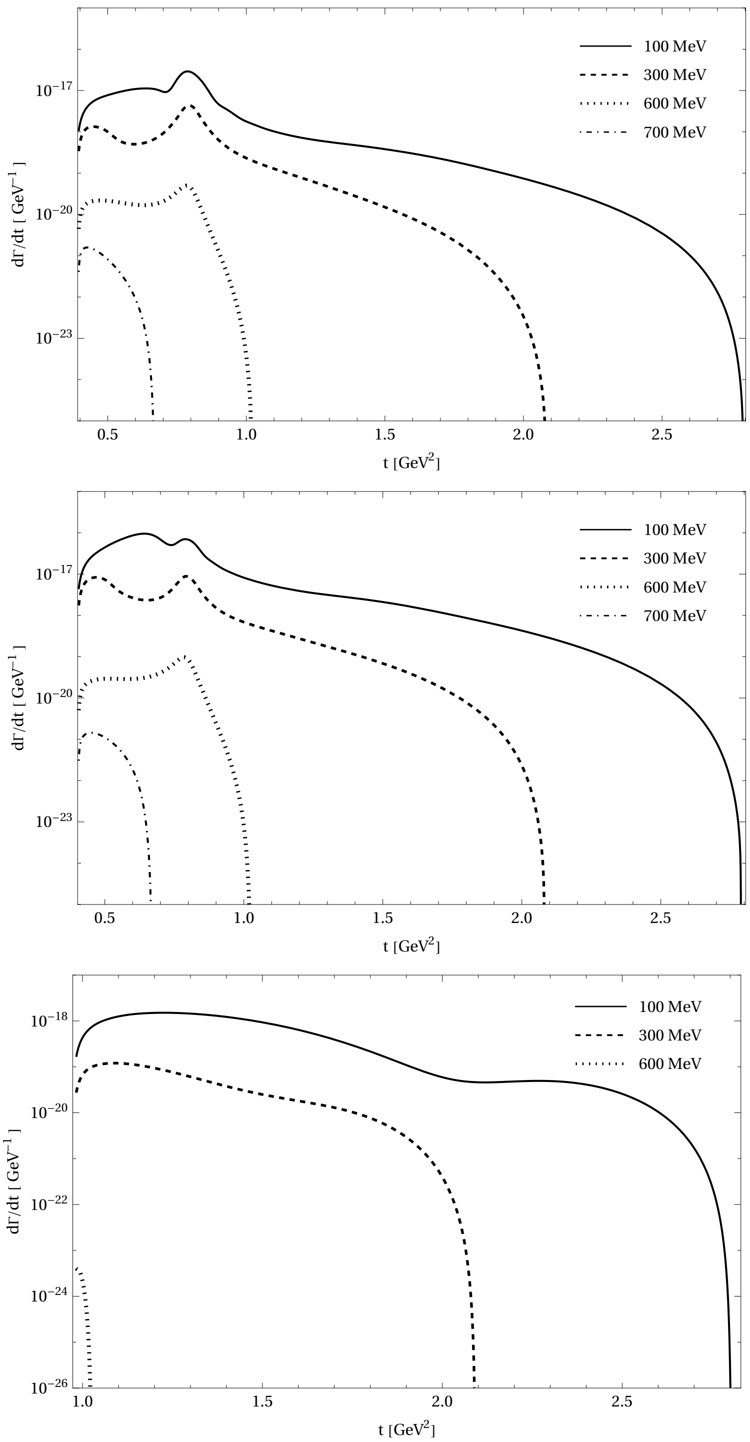

Figure 7. The $K^-\pi^0$ (top), $\bar{K}^0\pi^-$ (center) and K^-K^0 (bottom) SI hadronic invariant mass distributions for several $E_\gamma^{\rm cut}$ values.

$E_\gamma^{\rm cut}$	Br(Low)	BR(SI)	BR($F_V=\sqrt{2}F$) $\left[\mathcal{O}\left(p^4\right)\right]$	BR($F_V=\sqrt{3}F$) $\left[\mathcal{O}\left(p^4\right)\right]$
100 MeV	3.4×10^{-6}	3.0×10^{-6}	3.5×10^{-6}	3.8×10^{-6}
300 MeV	6.2×10^{-7}	3.4×10^{-7}	6.3×10^{-7}	9.4×10^{-7}
500 MeV	7.4×10^{-8}	3.5×10^{-8}	1.5×10^{-7}	3.3×10^{-7}

Table 1. Branching ratios Br($\tau^-\to K^-\pi^0\nu_\tau\gamma$) for different values of $E_\gamma^{\rm cut}$. The third column corresponds to the complete bremsstrahlung, and the fourth and fifth to the $\mathcal{O}\left(p^4\right)$ contributions.

$E_\gamma^{\rm cut}$	Br(Low)	BR(SI)	BR($F_V=\sqrt{2}F$) $\left[\mathcal{O}\left(p^4\right)\right]$	BR($F_V=\sqrt{3}F$) $\left[\mathcal{O}\left(p^4\right)\right]$
100 MeV	2.6×10^{-5}	1.4×10^{-5}	1.6×10^{-5}	1.6×10^{-5}
300 MeV	6.2×10^{-6}	1.1×10^{-6}	1.7×10^{-6}	1.9×10^{-6}
500 MeV	1.0×10^{-6}	7.1×10^{-8}	2.0×10^{-7}	2.4×10^{-7}

Table 2. Branching ratios Br($\tau^-\to\bar{K}^0\pi^-\nu_\tau\gamma$) for different values of $E_\gamma^{\rm cut}$. The third column corresponds to the complete bremsstrahlung, and the fourth and fifth to the $\mathcal{O}\left(p^4\right)$ contributions.

$E_\gamma^{\rm cut}$	BR(Low)	BR(SI)	BR($F_V=\sqrt{2}F$) $\left[\mathcal{O}\left(p^4\right)\right]$	BR($F_V=\sqrt{3}F$) $\left[\mathcal{O}\left(p^4\right)\right]$
100 MeV	5.3×10^{-7}	3.7×10^{-7}	6.8×10^{-7}	9.4×10^{-7}
300 MeV	4.8×10^{-8}	1.9×10^{-8}	1.7×10^{-7}	3.1×10^{-7}
500 MeV	3.7×10^{-10}	3.0×10^{-10}	1.1×10^{-8}	2.9×10^{-8}

Table 3. Branching ratios Br($\tau^-\to K^-K^0\nu_\tau\gamma$) for different values of $E_\gamma^{\rm cut}$. The third column corresponds to the complete bremsstrahlung, and the fourth and fifth to the $\mathcal{O}\left(p^4\right)$ contributions.

pression around the $K^*(892)$ peak, when the full distribution is compared to the Low one. The K^-K^0 invariant mass distribution is more sensitive to SD contributions, although the $\rho(1450)$ effect is hidden in the spectrum because of the corresponding kinematical suppression.

The photon energy distribution is shown in Fig. 9. The SI amplitude in all these decays governs the distribution for $E_\gamma\lesssim 100\,\text{MeV}$, in agreement with the outcomes for the branching ratio. However, the SD contributions become relevant for $E_\gamma\gtrsim 250$MeV. This feature makes these decays an excellent probe for testing SD effects. The above phenomenological analysis, for the $\tau^-\to\pi^-\pi^0\nu_\tau\gamma$ decays, can be found in Ref. [53], for instance.

4 Radiative Corrections

The overall differential decay width is given by

$$\left.\frac{d\Gamma}{dt}\right|_{PP(\gamma)}=\left.\frac{d\Gamma}{dt}\right|_{PP}+\left.\frac{d\Gamma}{dt}\right|_{\rm III}+\left.\frac{d\Gamma}{dt}\right|_{\rm IV/III}+\left.\frac{d\Gamma}{dt}\right|_{\rm rest}, \tag{4.1}$$

where the first term is the non-radiative differential width in Eq. (C.5), the second and third terms correspond to the Low approximation integrated according to the kinematics in Refs. [51, 53], Eq. (2.16), and the last term includes the remaining contributions.

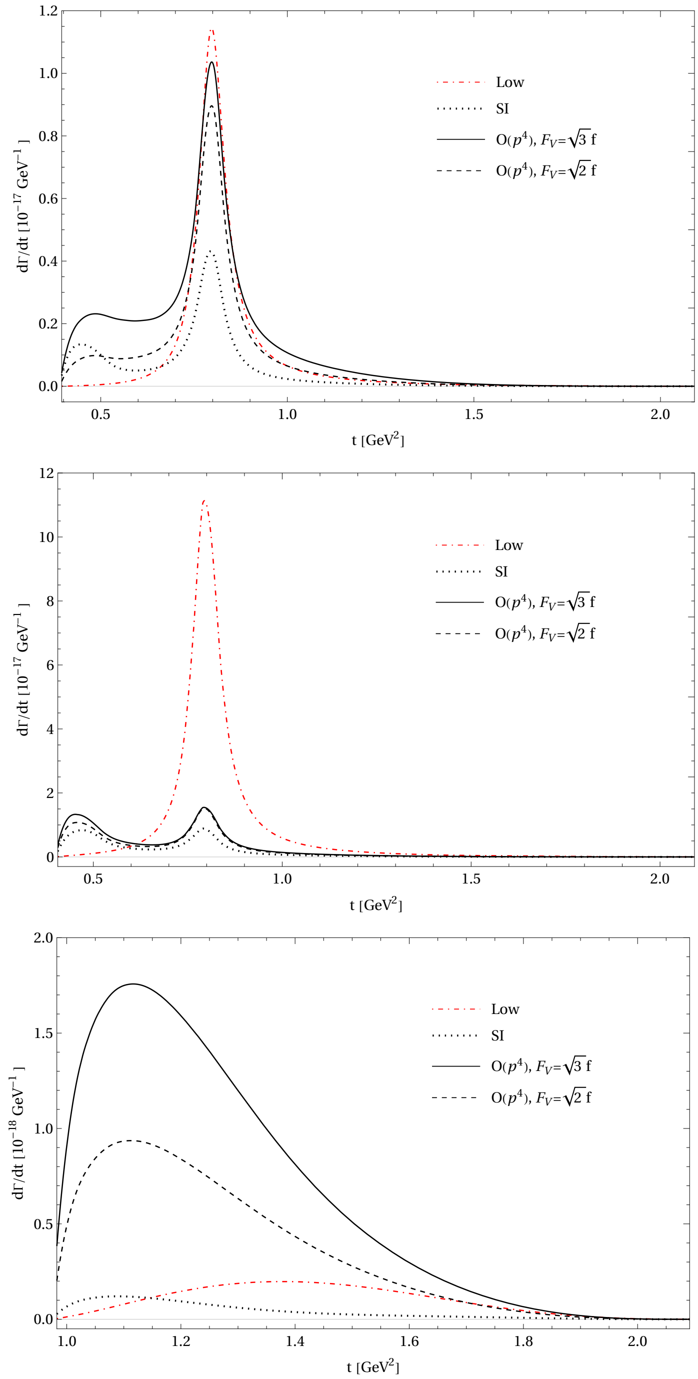

Figure 8. The $K^-\pi^0$ (top), $\bar{K}^0\pi^-$ (center) and K^-K^0 (bottom) hadronic invariant mass distributions for $E_\gamma^{\rm cut} \geq 300\,\text{MeV}$. The solid and dashed line represent the $\mathcal{O}\left(p^4\right)$ corrections using $F_V = \sqrt{3}F$ and $F_V = \sqrt{2}F$, respectively. The dotted line represents the bremsstrahlung contribution (SI). The red one corresponds to the Low approximation.

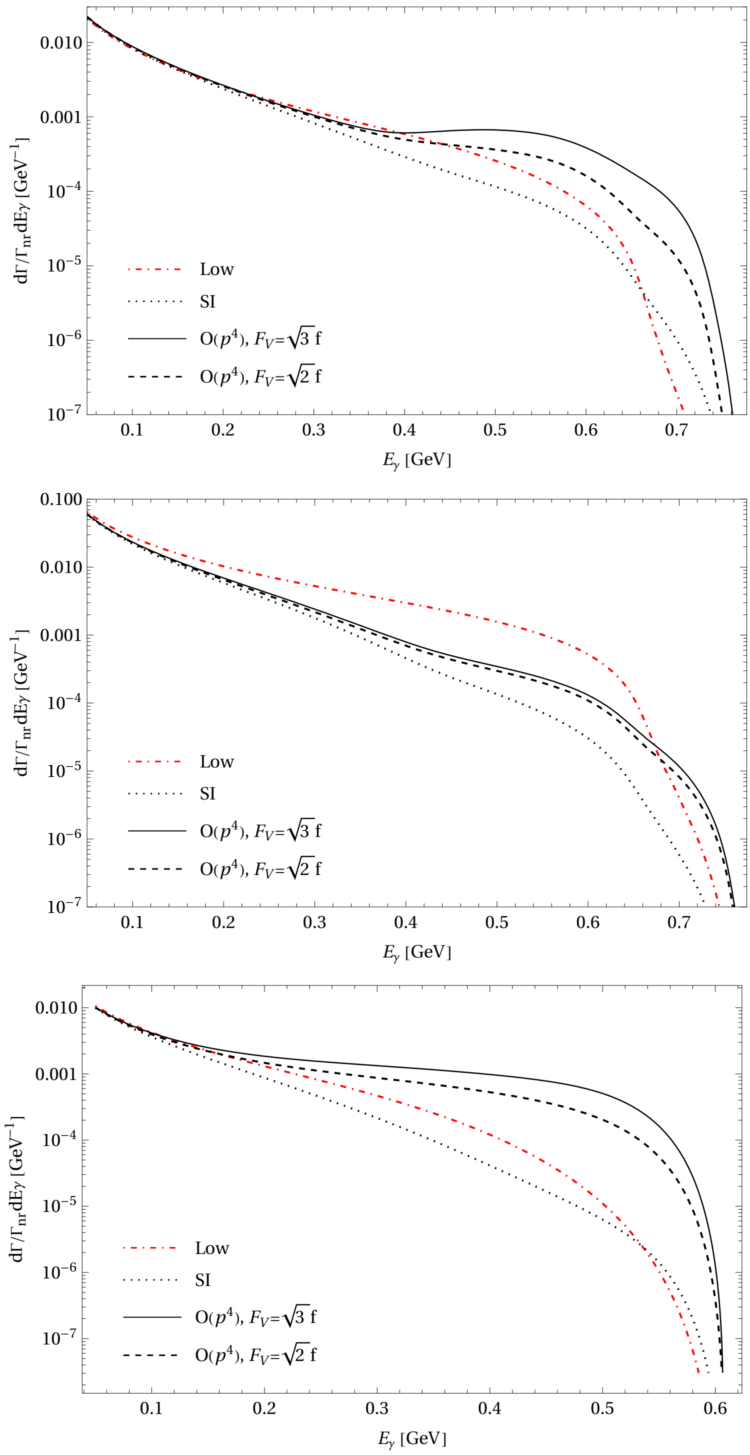

Figure 9. Photon energy distribution for the $\tau^- \to K^-\pi^0\nu_\tau\gamma$ (top), the $\tau^- \to \bar{K}^0\pi^-\nu_\tau\gamma$ (center) and the $\tau^- \to K^-K^0\nu_\tau\gamma$ (bottom) decays normalized with the non-radiative decay width. The dotted line represents the bremsstrahlung contribution. The solid and dashed lines represent the $\mathcal{O}\left(p^4\right)$ corrections using $F_V = \sqrt{3}F$ and $F_V = \sqrt{2}F$, respectively.

To evaluate the first term in Eq. (4.1) we use two models for the factorization of the radiative corrections to the form factors (FFs). In model 1, we factorize the corrections to the form factor [51] as

$$\tilde{F}_{+/0}(t,u) = \tilde{F}_{+/0}(t)\left[1+\delta F_{+/0}(t,u)\right] \ , \tag{4.2}$$

while in model 2, they are written as [11]

$$\tilde{F}_{+}(t,u) = \tilde{F}_{+}(t)\left\{1+\frac{\alpha}{4\pi}\left[2(m_-^2+m_\tau^2-u)\mathcal{C}(u,M_\gamma)+2\log\left(\frac{m_- m_\tau}{M_\gamma^2}\right)\right]\right\}+\delta\bar{f}_+(u) \tag{4.3}$$

$$\tilde{F}_0(t,u) \equiv \tilde{F}_+(t,u)+\frac{t}{\Delta_{-0}}\delta\bar{f}_-(u) \ , \tag{4.4}$$

where $\delta\bar{f}_+(u)$ and $\delta\bar{f}_-(u)$ are defined in Appx. B. A similar factorization prescription was used in Ref. [83] where model 2 was preferred over model 1 for the $K_{\mu 3}$ decays since the loop contributions to $f_{+/-}(u)$ are different [4]. We will see here that model 1 factorization warrants smoother corrections than model 2 when resonance contributions are included, as resonance enhancements will cancel in the long-distance radiative correction factor $G_{\rm EM}(t)$ in Eq. (4.5), as opposed to model 2. This motivates our preference of model 1 over model 2 in our following phenomenological analysis.

The correction factors $\widetilde{\delta}_A(t)$ and $\overline{\delta}_A(t)$, where $A=+,0,+0$, are both IR divergent when $M_\gamma \to 0$, nevertheless, the overall contribution, $\delta_A(t)=\overline{\delta}_A(t)+\widetilde{\delta}_A(t)$, is finite. In Fig. 10, we can see the predictions for $\delta_A(t)$ for the $K^-\pi^0$, $\bar{K}^0\pi^-$, and K^-K^0 decay modes using the FFs in model 1 and 2. Whilst our results for $\delta_+(t)$ in model 2 agree with those in Ref. [11] in Figure 2, the predictions for $\delta_0(t)$ are slightly different as a consequence of the parameterization of the scalar form factor [5].

The differential decay width can be written as

$$\begin{aligned}\left.\frac{d\Gamma}{dt}\right|_{PP(\gamma)} =& \frac{G_F^2\left|V_{uD}F_+(0)\right|^2 S_{\rm EW} m_\tau^3}{768\pi^3 t^3}\left(1-\frac{t}{m_\tau^2}\right)^2 \lambda^{1/2}(t,m_-^2,m_0^2) \\ &\times\left[C_V^2|\tilde{F}_+(t)|^2\left(1+\frac{2t}{m_\tau^2}\right)\lambda(t,m_-^2,m_0^2)+3C_S^2\Delta_{-0}^2|\tilde{F}_0(t)|^2\right]G_{\rm EM}(t) \ ,\end{aligned} \tag{4.5}$$

where $G_{\rm EM}(t)$ encodes the electromagnetic corrections due to real and virtual photons. For simplicity, we have splitted $G_{\rm EM}(t)$ in two parts: the leading Low approximation plus non-radiative contributions, $G_{\rm EM}^{(0)}(t)$, and the remainder, $\delta G_{\rm EM}(t)$, which includes the SD contributions to the amplitude. The predictions for both are shown in Fig. 11.

[4] Both prescriptions were studied for the K_{e3} decays in Ref. [68], their outcomes for $\delta_{\rm EM}^{K\ell}(\mathcal{D}_3)(\%)$ are shifted from 0.41 to 0.56 for K_{e3}^0 and from -0.564 to -0.410 for $K_{e3}^\pm$ modes where the former numbers correspond to model 2.

[5] This effect is mainly responsible for the slight difference between our results for model 2 in Table 10 and those in Ref. [11].

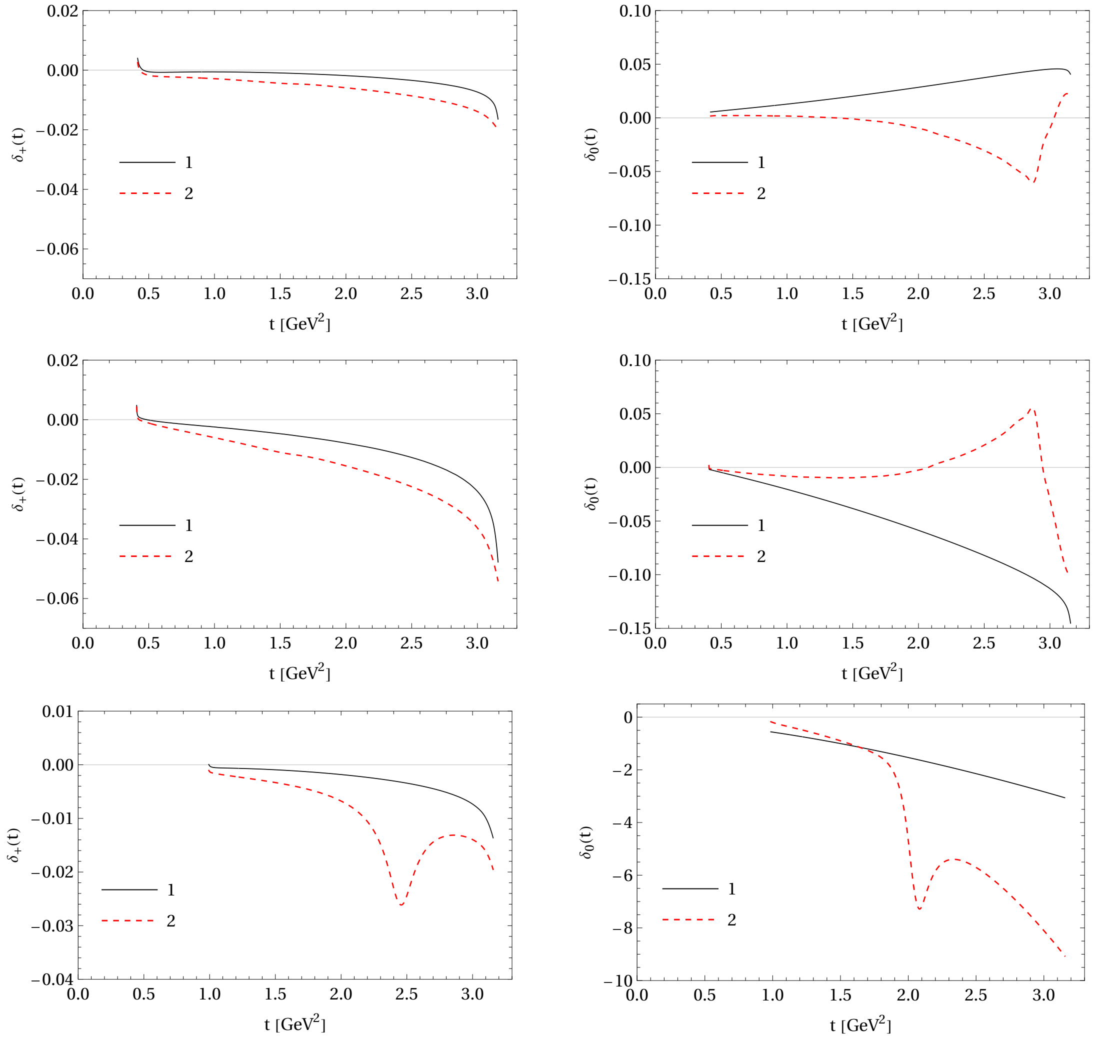

Figure 10. Correction factors $\delta_+^{\mathrm{EM}}(t)$ (left) and $\delta_0^{\mathrm{EM}}(t)$ (right) to the differential decay rates of the $K^-\pi^0$, $\bar{K}^0\pi^-$ and K^-K^0 modes from top to bottom, according to models 1 (solid black) and 2 (dashed red).

Integrating upon t, we get

$$\Gamma_{PP(\gamma)} = \frac{G_F^2 S_{\mathrm{EW}} m_\tau^5}{96\pi^3} |V_{uD}F_+(0)|^2 I_{PP}^\tau \left(1+\delta_{\mathrm{EM}}^{PP}\right)^2 , \tag{4.6}$$

where

$$\begin{aligned} I_{PP}^\tau =& \frac{1}{8m_\tau^2}\int_{t_{\mathrm{thr}}}^{m_\tau^2} \frac{dt}{t^3}\left(1-\frac{t}{m_\tau^2}\right)^2 \lambda^{1/2}(t,m_-^2,m_0^2) \\ &\times \left[C_V^2|\tilde{F}_+(t)|^2\left(1+\frac{2t}{m_\tau^2}\right)\lambda(t,m_-^2,m_0^2) + 3C_S^2\Delta_{-0}^2|\tilde{F}_0(t)|^2\right] . \end{aligned} \tag{4.7}$$

The results for $\delta_{\mathrm{EM}}^{PP}$ are shown in Table 4, where the second and third columns cor-

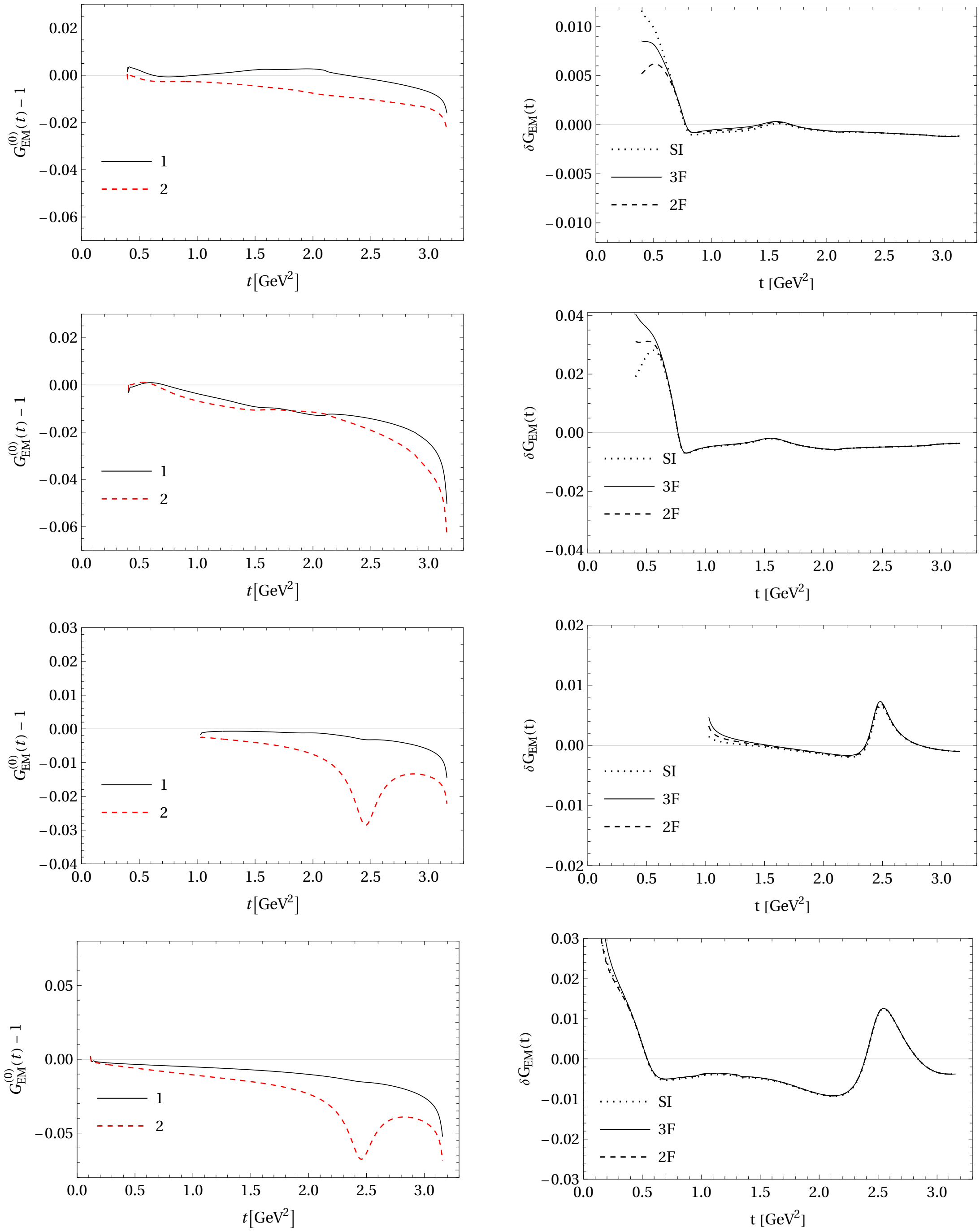

Figure 11. Correction factors $G_{\rm EM}^{(0)}(t)$ (left) and $\delta G_{\rm EM}(t)$ (right) to the differential decay rates of the $K^-\pi^0$, $\bar{K}^0\pi^-$, K^-K^0, and $\pi^-\pi^0$ modes from top to bottom.

$\delta_{\rm EM}$	Ref. [11]	Model 1	Model 2	$\mathcal{D}^{\rm IV/III}$	SI	2F	3F
$K^-\pi^0$	$-0.20(20)$	-0.019	-0.137	$+1.3\cdot10^{-4}$	-0.001	$+0.006$	$+0.010$
$\bar{K}^0\pi^-$	$-0.15(20)$	-0.086	-0.208	$+1.5\cdot10^{-5}$	-0.098	-0.085	-0.080
K^-K^0	–	-0.046	-0.223	$+9.5\cdot10^{-5}$	-0.012	$+0.003$	$+0.016$
$\pi^-\pi^0$	–	-0.196	-0.363	$+9.4\cdot10^{-5}$	-0.010	-0.002	$+0.010$

Table 4. Electromagnetic corrections to hadronic τ decays in %.

respond to the first and second terms in Eq. (4.1), the fourth column to the third term and the last three columns to the fourth term in that equation. The value in model 1 for the $\bar{K}^0\pi^-$ channel agrees with the result in Ref. [56], which is related to our definition by $\delta_{\rm EM}=\delta_{\rm EM}^{\rm m.i.}/2\simeq-0.063\%$. Although our outcomes for the $(K\pi)^-$ modes agree within errors with those in Refs. [11, 56], the value in model 2 (and also model 1) for the $K^-\pi^0$ decay channel is larger than the $K^0\pi^-$ one, which is at odds with Ref. [11][6].

The complete radiative corrections (that we always quote in %) are obtained adding to the model 1/2 results, the (negligible) $\mathcal{D}^{\rm IV/III}$ part and the $2F/3F$ contributions (which include the SI part). We explained before why we preferred the model 1 over the model 2 results. We will take the difference with respect to model 2 as an asymmetric error on the model 1 results. For the structure-dependent contributions, we consider the $3F$ results as our central values and the difference with respect to $2F$ as a symmetric error for our model-dependence. To be on the safe side, we will take twice this error as our corresponding uncertainty. Proceeding this way, our main results are

$$\begin{aligned}
\delta^{K^-\pi^0} &= -\left(0.009^{+0.008}_{-0.118}\right)\,, & \delta^{\bar{K}^0\pi^-} &= -\left(0.166^{+0.010}_{-0.122}\right)\,,\\
\delta^{K^-K^0} &= -\left(0.030^{+0.026}_{-0.179}\right)\,, & \delta^{\pi^-\pi^0} &= -\left(0.186^{+0.024}_{-0.169}\right)\,.
\end{aligned}\tag{4.8}$$

We see that the model-independent contributions are responsible for the relatively large radiative corrections obtained for the $(\bar{K}/\pi)^0\pi^-$ modes. The dominant (asymmetric) uncertainty comes from the difference between the model 1/2 results, which is much larger than the deviation between the model-dependent $2F/3F$ values. Our results for the $\delta^{K^-\pi^0/\bar{K}^0\pi^-}$ agree with those in Ref. [11], and we reduce the uncertainty band by $\sim45\%$. We note that the estimate of the errors in this reference yields also an uncertainty band in agreement with ours for $\delta^{K^-K^0/\pi^-\pi^0}$ (our errors are smaller by a factor ~ 2 again). Although our $\delta^{K^-\pi^0}$ and $\delta^{\bar{K}^0\pi^-}$ seem to differ (the main reason being the scaling of the inner bremsstrahlung contribution with the inverse of the charged meson mass), the corresponding significance of their non-equality is only $\sim0.7\sigma$, according to our uncertainties. We understand that the radiative corrections in Eq. (4.8) constitute the state-of-the-art results and, as such, should be employed in precision analysis like, e.g. CKM unitarity or lepton universality tests [84] and searches for non-standard interactions.

For completeness, we have also evaluated these corrections for the $K^-\eta^{(\prime)}$ modes. In the $G_{\rm EM}^{(0)}$ approximation and using the respective dominance of the vector (scalar) form

[6] Incidentally, our results would agree more closely swapping the numbers for $\delta_{\rm EM}^{K^-\tau}\leftrightarrow\delta_{\rm EM}^{\bar{K}^0\tau}$ in Ref. [11].

factor [13], we obtain

$$\delta^{K^-\eta} = -\left(0.026^{+0.024}_{-0.162}\right) \ , \qquad \delta^{K^-\eta'} = -\left(0.304^{+0.380}_{-0.030}\right) \ , \tag{4.9}$$

where the uncertainty is saturated by the difference between the model 1/2 results. The $K^-\eta'$ decay mode is the only one (completely) dominated by the scalar form factor, which causes the relatively large magnitude of the corresponding radiative correction.

5 Conclusions

Radiative corrections to the one-meson tau decays have been employed in CKM unitarity, lepton universality and non-standard interactions tests. The corresponding results for the dipion tau decays allowed tau-based computations of the leading-order piece of the hadronic vacuum polarization part of the muon $g-2$. Even though the model-independent part of these corrections was available for the $K\pi$ modes, the structure-dependent one remained to be calculated. We have filled this gap, enabling a computation of the corresponding radiative correction factors with reduced uncertainties. For completeness, we also quote these results for the PP ($P=\pi, K$) modes and estimate them for the $K\eta^{(\prime)}$ cases.

A $K_{\ell 3}$ decays

The most general amplitude for the $K(p_K) \to \pi(p_\pi)\ell(P)\nu_\ell(q)\gamma(k)$ decays that complies with Lorentz invariance and the discrete symmetries of QCD can be written as

$$\begin{aligned}\mathcal{M} =& \frac{eG_F V_{us}^*}{\sqrt{2}}\epsilon_\mu^* \left[\frac{H_\nu(-p_K,p_\pi)}{k^2+2k\cdot P}\bar{u}(q)\gamma^\nu(1-\gamma^5)(m_\ell - \not{P} - \not{k})\gamma^\mu v(P)\right.\\ &\left.+(V^{\mu\nu}-A^{\mu\nu})\bar{u}(q)\gamma_\nu(1-\gamma^5)v(P)\right] \ ,\end{aligned} \tag{A.1}$$

where

$$\begin{aligned}H^\nu(-p_K,p_\pi) &\equiv \langle \pi(p_\pi)\,|\bar{s}\gamma^\nu u|\,K(p_K)\rangle\\ &= -C_V F_+(t)\left[(p_K+p_\pi)^\nu - \frac{\Delta_{K\pi}}{t}(p_K-p_\pi)^\nu\right] - C_S\frac{\Delta_{K\pi}}{t}(p_K-p_\pi)^\nu F_0(t) \ ,\end{aligned} \tag{A.2}$$

with $t=(p_K-p_\pi)^2$.

The structure-independent term is given by

$$
\begin{aligned}
V_{\rm SI}^{\mu\nu} =& \frac{H^\nu(-p_K+k,p_\pi)(k-2p_K)^\mu}{k^2-2k\cdot p_K} + \left\{-C_V F_+(t') - \frac{\Delta_{K\pi}}{t'}\left[C_S F_0(t') - C_V F_+(t')\right]\right\} g^{\mu\nu} \\
&+ C_V \frac{F_+(t')-F_+(t)}{k\cdot(p_K-p_\pi)}\left[(p_K+p_\pi)^\nu - \frac{\Delta_{K\pi}}{t}(p_K-p_\pi)^\nu\right](p_K-p_\pi)^\mu \\
&+ \frac{\Delta_{K\pi}}{tt'}\left\{2\left[C_S F_0(t') - C_V F_+(t')\right] + \frac{C_S t'}{k\cdot(p_K-p_\pi)}\left[F_0(t')-F_0(t)\right]\right\} \\
&\times (p_K-p_\pi)^\mu (p_K-p_\pi)^\nu \ ,
\end{aligned}
\tag{A.3}
$$

where $C_V^{K^-\pi^0} = C_S^{K^-\pi^0} = 1/\sqrt{2}$ for $K^+ \to \pi^0 \ell^+ \nu_\ell \gamma$, and

$$
\begin{aligned}
V_{\rm SI}^{\mu\nu} =& \frac{H^\nu(-p_K,p_\pi+k)(k+2p_\pi)^\mu}{k^2+2k\cdot p_\pi} + \left\{C_V F_+(t') - \frac{\Delta_{K\pi}}{t'}\left[C_S F_0(t') - C_V F_+(t')\right]\right\} g^{\mu\nu} \\
&+ C_V \frac{F_+(t')-F_+(t)}{k\cdot(p_K-p_\pi)}\left[(p_K+p_\pi)^\nu - \frac{\Delta_{K\pi}}{t}(p_K-p_\pi)^\nu\right](p_K-p_\pi)^\mu \\
&+ \frac{\Delta_{K\pi}}{tt'}\left\{2\left[C_S F_0(t') - C_V F_+(t')\right] + \frac{C_S t'}{k\cdot(p_K-p_\pi)}\left[F_0(t')-F_0(t)\right]\right\} \\
&\times (p_K-p_\pi)^\mu (p_K-p_\pi)^\nu \ ,
\end{aligned}
\tag{A.4}
$$

where $C_V^{\bar{K}^0\pi^-} = C_S^{\bar{K}^0\pi^-} = 1$ for $K^0 \to \pi^- \ell^+ \nu_\ell \gamma$, both with $t' \equiv (p_K - p_\pi - k)^2$. We recover the Eqs. (2.3) and (2.4) by replacing $\left\{\begin{smallmatrix} P \\ p_K \end{smallmatrix}\right\} \to \left\{\begin{smallmatrix} -P \\ -p_K \end{smallmatrix}\right\}$ and $m_\ell \to m_\tau$. The structure-dependent terms are analogous to those in Eqs. (2.5) and (2.6).

At $\mathcal{O}(p^0)$, we get

$$
V_{\rm SI}^{\mu\nu} = -C_{K^+}\frac{p_K^\mu}{k\cdot p_K}(p_K+p_\pi)^\nu - C_{K^+}\left(g^{\mu\nu} - \frac{p_K^\mu k^\nu}{k\cdot p_K}\right) \ , \tag{A.5}
$$

for $K^+ \to \pi^0$, and

$$
V_{\rm SI}^{\mu\nu} = -C_{K^0}\frac{p_\pi^\mu}{k\cdot p_\pi}(p_K+p_\pi)^\nu + C_{K^0}\left(g^{\mu\nu} - \frac{p_\pi^\mu k^\nu}{k\cdot p_\pi}\right) \ , \tag{A.6}
$$

for $K^0 \to \pi^-$, where $C_K = C_S = C_V$. Thus, the overall amplitude at $\mathcal{O}(p^0)$ is given by

$$
\mathcal{M}_\gamma = \frac{eG_F}{\sqrt{2}} V_{us}^* C_{K^+} \bar{u}(q)(1+\gamma^5)(2\not{p}_\pi - m_\ell)\left(\frac{\epsilon\cdot P}{k\cdot P} - \frac{\epsilon\cdot p_K}{k\cdot p_K} + \frac{\not{k}\not{\epsilon}}{2k\cdot P}\right) v(P) \ , \tag{A.7}
$$

and

$$
\mathcal{M}_\gamma = \frac{eG_F}{\sqrt{2}} V_{us}^* C_{K^0} \bar{u}(q)(1+\gamma^5)(2\not{p}_K + m_\ell)\left(\frac{\epsilon\cdot P}{k\cdot P} - \frac{\epsilon\cdot p_\pi}{k\cdot p_\pi} + \frac{\not{k}\not{\epsilon}}{2k\cdot P}\right) v(P) \ . \tag{A.8}
$$

These two expressions agree with the Eqs. (13) and (14) in Ref. [68]. To this order, $V^{\mu\nu}_{\rm SD}$ and $A^{\mu\nu}_{\rm SD}$, which are $\mathcal{O}(p^2)$, can be neglected.

In the Low limit, we obtain

$$\mathcal{M}_\gamma = \frac{eG_F V_{us}^*}{\sqrt{2}}\bar{u}(q)\gamma_\nu(1-\gamma^5)v(P)H^\nu(-p_K,p_\pi)\left(\frac{\epsilon\cdot p_+}{k\cdot p_+}-\frac{\epsilon\cdot P}{k\cdot P}\right) , \tag{A.9}$$

where the subscript $+$ refers to the charged meson. The spin-averaged squared matrix element is then given by

$$\begin{aligned}\overline{|\mathcal{M}_\gamma|^2} =&4C_K^2e^2G_F^2\left|V_{us}\right|^2 S_{\rm EW}^K\left\{\left[\frac{m_\ell^2}{2}(t-m_\ell^2)+2m_K^2m_\pi^2+2u(m_\ell^2-t+m_K^2+m_\pi^2)-2u^2\right.\right.\\ &\left.-\frac{\Delta_{K\pi}}{t}m_\ell^2(2u+t-m_\ell^2-2m_\pi^2)+\frac{\Delta_{K\pi}^2}{t^2}\frac{m_\ell^2}{2}(t-m_\ell^2)\right]|F_+(t)|^2\\ &+\frac{\Delta_{K\pi}m_\ell^2}{t}\left[2u+t-m_\ell^2-2m_\pi^2+\frac{\Delta_{K\pi}}{t}(m_\ell^2-t)\right]{\rm Re}\left[F_+(t)F_0^*(t)\right]\\ &\left.+\frac{\Delta_{K\pi}^2m_\ell^2}{2t^2}\left(t-m_\ell^2\right)|F_0(t)|^2\right\}\sum_{\gamma\ \rm pols.}\left|\frac{p_-\cdot\epsilon}{p_-\cdot k}-\frac{P\cdot\epsilon}{P\cdot k}\right|^2+\mathcal{O}(k^0) ,\end{aligned} \tag{A.10}$$

where $u=(p_K-P)^2$. The last expression can also be written in terms of $f_{+/-}(t)$,

$$\overline{|\mathcal{M}_\gamma|^2} = 2C_K^2m_K^4e^2G_F^2\left|V_{us}\right|^2 S_{\rm EW}^K\rho^{(0)}(y,z)\sum_{\gamma\ \rm pols.}\left|\frac{p_-\cdot\epsilon}{p_-\cdot k}-\frac{P\cdot\epsilon}{P\cdot k}\right|^2+\mathcal{O}(k^0) , \tag{A.11}$$

where

$$\rho^{(0)}(y,z) = A_1^{(0)}(y,z)\left|f_+(t)\right|^2+A_2^{(0)}(y,z){\rm Re}\left[f_+(t)f_-^*(t)\right]+A_3^{(0)}(y,z)\left|f_-(t)\right|^2 , \tag{A.12}$$

and the kinematical densities are

$$A_1^{(0)} = 4(y+z-1)(1-y)+r_\ell(4y+3z-3)-4r_\pi+r_\ell(r_\pi-r_\ell) , \tag{A.13a}$$

$$A_2^{(0)} = 2r_\ell(r_\ell-r_\pi-2y-z+3) , \tag{A.13b}$$

$$A_3^{(0)} = r_\ell(r_\pi-r_\ell+1-z) , \tag{A.13c}$$

with

$$z=\frac{2p_\pi\cdot p_K}{m_K^2}=\frac{2E_\pi}{m_k} , \qquad y=\frac{2p_K\cdot p_\ell}{m_K^2}=\frac{2E_\ell}{m_k} , \tag{A.14}$$

$r_\ell=(m_\ell/m_K)^2$, and $r_\pi=(m_\pi/m_K)^2$. Here, E_π (E_ℓ) is the energy of the pion (charged lepton) in the kaon rest frame. The expression in Eq. (A.11) can be compared directly with the results in Refs. [68, 83, 85].

The $K \to \pi \ell \nu_\ell$ decay width without radiative corrections [11] is given by

$$\Gamma(K \to \pi \ell \nu_\ell) = \frac{G_F^2 m_K^5}{192\pi^3} S_{\rm EW}^K |V_{us}|^2 |F_+(0)| I_K^\ell \ , \tag{A.15}$$

where

$$\begin{aligned} I_K^\ell = &\int_{m_\ell^2}^{t_{\max}} dt \frac{1}{m_K^8} \lambda^{3/2}(t, m_K^2, m_\pi^2) \left(1 - \frac{m_\ell^2}{t}\right)^2 \left(1 + \frac{m_\ell^2}{2t}\right) \\ &\times \left[C_V^2 |\tilde{F}_+(t)|^2 + \frac{3\Delta_{K\pi}^2 m_\ell^2}{(2t + m_\ell^2)\lambda(t, m_K^2, m_\pi^2)} C_S |\tilde{F}_0(t)|^2\right] \ , \end{aligned} \tag{A.16}$$

and $t_{\max} = (m_K - m_\pi)^2$.

B Virtual corrections to the hadronic tau decays

The radiative corrections to the $\tau^- \to (P_1 P_2)^- \nu_\tau$ decays at $\mathcal{O}(p^2)$ in Chiral Perturbation Theory [86–88] are depicted in Fig. 12. The overall contribution is given by [50]

$$\delta H^\mu(t, u) = C_V \delta f_+(u) (p_1 - p_0)^\mu + C_V \delta f_-(u) (p_1 + p_0)^\mu \ , \tag{B.1}$$

where

$$\begin{aligned} \delta f_+(u) =& \frac{\alpha}{4\pi} \left[2 + \frac{1}{\epsilon} - \gamma_E + \log 4\pi - \log \frac{m_\tau^2}{\mu^2} + (u - m_-^2)\mathcal{A}(u) + (u - m_-^2 - m_\tau^2)\mathcal{B}(u)\right. \\ &\left. + 2(m_-^2 + m_\tau^2 - u)\mathcal{C}(u, M_\gamma) + 2\log\left(\frac{m_- m_\tau}{M_\gamma^2}\right)\right] , \end{aligned} \tag{B.2}$$

$$\begin{aligned} \delta f_-(u) =& \frac{\alpha}{4\pi} \left[-5 - 3\left(\frac{1}{\epsilon} - \gamma_E + \log 4\pi\right) + \log \frac{m_-^2}{\mu^2} + 2\log \frac{m_\tau^2}{\mu^2} + (3u + m_-^2 - 2m_\tau^2)\mathcal{A}(u)\right. \\ &\left. + (u + m_-^2 - m_\tau^2)\mathcal{B}(u)\right] \ , \end{aligned} \tag{B.3}$$

$$\mathcal{A}(u) = \frac{1}{u} \left(-\frac{1}{2} \log r_\tau + \frac{2 - y}{\sqrt{r_\tau}} \frac{x}{1 - x^2} \log x\right) \ , \tag{B.4}$$

$$\mathcal{B}(u) = \frac{1}{u} \left(\frac{1}{2} \log r_\tau + \frac{2r_\tau - y}{\sqrt{r_\tau}} \frac{x}{1 - x^2} \log x\right) \ , \tag{B.5}$$

$$\begin{aligned} \mathcal{C}(u, M_\gamma) =& \frac{1}{m_\tau m_-} \frac{x}{1 - x^2} \left[-\frac{1}{2} \log^2 x + 2\log x \log(1 - x^2) - \frac{\pi^2}{6} + \frac{1}{8} \log^2 r_\tau\right. \\ &\left. + \mathrm{Li}_2(x^2) + \mathrm{Li}_2\left(1 - \frac{x}{\sqrt{r_\tau}}\right) + \mathrm{Li}_2(1 - x\sqrt{r_\tau}) - \log x \log\left(\frac{M_\gamma^2}{m_\tau m_-}\right)\right] \ , \end{aligned} \tag{B.6}$$

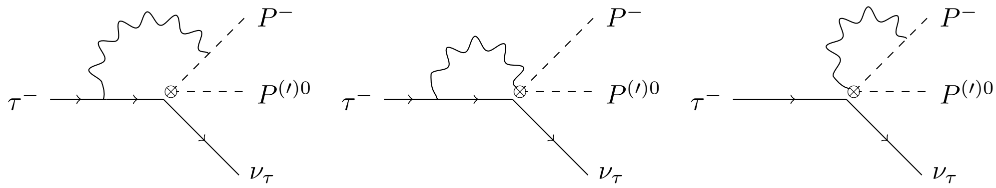

Figure 12. Photon loop diagrams that contribute to the $\tau^- \to (P_1P_2)^-\nu_\tau$ decays.

and $C_V^{\pi\pi,KK,K^-\pi^0,K^0\pi^-} = \left(\sqrt{2}, -1, \frac{1}{\sqrt{2}}, -1\right)$. Here, $\mathcal{A}(u)$, $\mathcal{B}(u)$ and $\mathcal{C}(u, M_\gamma)$ are written in terms of the variables

$$r_\tau = \frac{m_\tau^2}{m_-^2} \ , \qquad y = 1 + r_\tau - \frac{u}{m_-^2} \ , \qquad x = \frac{1}{2\sqrt{r_\tau}}\left(y - \sqrt{y^2 - 4r_\tau}\right) \ , \tag{B.7}$$

and the dilogarithm

$$\mathrm{Li}_2(x) = -\int_0^1 \frac{dt}{t}\log(1 - xt) \ . \tag{B.8}$$

The radiative corrections to these decays induce a dependence in the u variable. From a comparison with the results in Ref. [11], we get the following relation

$$\begin{aligned} \delta\bar{f}_+(u) &= \frac{\alpha}{4\pi}\frac{1}{f_+(0)}\left[\Gamma_1(u, m_\tau^2, m_-^2) + \Gamma_2(u, m_\tau^2, m_-^2)\right] + \cdots \\ &= \frac{\alpha}{4\pi}\frac{1}{f_+(0)}\left[(u - m_-^2)\mathcal{A}(u) + (u - m_-^2 - m_\tau^2)\mathcal{B}(u)\right] + \cdots \ , \end{aligned} \tag{B.9}$$

and

$$\begin{aligned} \delta\bar{f}_-(u) &= \frac{\alpha}{4\pi}\frac{1}{f_+(0)}\left[\Gamma_1(u, m_\tau^2, m_-^2) - \Gamma_2(u, m_\tau^2, m_-^2)\right] + \cdots \\ &= \frac{\alpha}{4\pi}\frac{1}{f_+(0)}\left[(3u + m_-^2 - 2m_\tau^2)\mathcal{A}(u) + (u + m_-^2 - m_\tau^2)\mathcal{B}(u)\right] + \cdots \ . \end{aligned} \tag{B.10}$$

C $\tau^- \to (P_1P_2)^-\nu_\tau$ decays

After the inclusion of the virtual-photon radiative corrections to the form factor in Sect. B, the amplitude for the $\tau^-(P) \to P_1^-(p_-)P_2^0(p_0)\nu_\tau(q)$ decays is given by

$$\mathcal{M}_0 = \frac{G_F V_{uD}\sqrt{S_{\mathrm{EW}}}}{\sqrt{2}} H_\nu(p_-, p_0)\bar{u}(q)\gamma^\nu(1 - \gamma^5)u(P) \ . \tag{C.1}$$

Thus, the spin-averaged squared amplitude follows

$$\begin{aligned} \overline{|\mathcal{M}_0|^2} =& 2G_F^2 |V_{uD}|^2 S_{\mathrm{EW}} \Big\{ C_S^2 |F_0(t,u)|^2 D_0^{P^-P^0}(t,u) \\ &+ C_S C_V \mathrm{Re}\left[F_+(t,u)F_0^*(t,u)\right] D_{+0}^{P^-P^0}(t,u) + C_V^2 |F_+(t,u)|^2 D_+^{P^-P^0}(t,u) \Big\} \ , \end{aligned} \tag{C.2}$$

where we have defined $F_{+/0}(t,u) = F_{+/0}(t) + \delta F_{+/0}(t,u)$, and $\delta F_0(t,u) \equiv \delta F_+(u) + \frac{t}{\Delta_{-0}}\delta F_-(u)$. The expressions for $D_0^{P^-P^0}(t,u)$, $D_{+0}^{P^-P^0}(t,u)$ and $D_+^{P^-P^0}(t,u)$ are given in Eqs. (2.10-2.12).

The differential decay width in the tau rest frame is

$$\frac{d^2\Gamma}{dtdu} = \frac{1}{32(2\pi)^3 m_\tau^3}\overline{|\mathcal{M}_0|^2} \,, \tag{C.3}$$

where $t = (p_- + p_0)^2$ is the invariant mass and $u = (P - p_-)^2 = (p_0 + q)^2$. The physical region is limited by $(m_- + m_0)^2 \le t \le m_\tau^2$ and $u^-(t) \le u \le u^+(t)$, with

$$u^\pm(t) = \frac{1}{2t}\left[2t(m_\tau^2 + m_0^2 - t) - (m_\tau^2 - t)(t + m_-^2 - m_0^2) \pm (m_\tau^2 - t)\sqrt{\lambda(t, m_-^2, m_0^2)}\right] \,, \tag{C.4}$$

and $\lambda(x,y,z) = x^2 + y^2 + z^2 - 2xy - 2xz - 2yz$.

The invariant mass distribution is obtained integrating upon the u variable

$$\begin{aligned}\frac{d\Gamma}{dt} =& \frac{G_F^2 S_{\mathrm{EW}}|V_{uD}|^2 m_\tau^3}{384\pi^3 t}\left\{\frac{1}{2t^2}\left(1 - \frac{t}{m_\tau^2}\right)^2 \lambda^{1/2}(t, m_-^2, m_0^2)\right.\\ &\times\left[C_V^2\,|F_+(t)|^2\left(1 + \frac{2t}{m_\tau^2}\right)\lambda(t, m_-^2, m_0^2)\left(1 + \tilde{\delta}_+(t)\right) + 3C_S^2\Delta_{-0}^2\,|F_0(t)|^2\left(1 + \tilde{\delta}_0(t)\right)\right]\\ &\left.+C_S C_V \frac{4}{\sqrt{t}}\tilde{\delta}_{+0}(t)\right\} \,,\end{aligned} \tag{C.5}$$

where

$$\tilde{\delta}_0(t) = \frac{\int_{u^-(t)}^{u^+(t)} D_0^{P^-P^0}(t,u) 2\mathrm{Re}\left[F_0(t)\delta F_0^*(t,u)\right] du}{\int_{u^-(t)}^{u^+(t)} D_0^{P^-P^0}(t,u)|F_0(t)|^2 du} \,, \tag{C.6}$$

$$\tilde{\delta}_+(t) = \frac{\int_{u^-(t)}^{u^+(t)} D_+^{P^-P^0}(t,u) 2\mathrm{Re}\left[F_+(t)\delta F_+^*(u)\right] du}{\int_{u^-(t)}^{u^+(t)} D_+^{P^-P^0}(t,u)|F_+(t)|^2 du} \,, \tag{C.7}$$

$$\tilde{\delta}_{+0}(t) = \frac{3t\sqrt{t}}{4m_\tau^6}\int_{u^-(t)}^{u^+(t)} D_{+0}^{P^-P^0}(t,u)\left(\mathrm{Re}\left[F_+(t)\delta F_0^*(t,u)\right] + \mathrm{Re}\left[F_0(t)\delta F_+^*(u)\right]\right) du \,. \tag{C.8}$$

D Kinematics

As in Refs. [11, 51, 53, 89], after an integration over $\mathcal{D}_{\mathrm{IV/III}}$ and $\mathcal{D}_{\mathrm{III}}$, the functions in Eqs. (2.15) are given by

$$\begin{aligned}J_{11}(t,u) =& \log\left(\frac{2x_+(t,u)\bar{\gamma}}{M_\gamma}\right)\frac{1}{\bar{\beta}}\log\left(\frac{1+\bar{\beta}}{1-\bar{\beta}}\right)\\ &+\frac{1}{\bar{\beta}}\left[\mathrm{Li}_2(1/Y_2) - \mathrm{Li}_2(Y_1) + \log^2(-1/Y_2)/4 - \log^2(-1/Y_1)/4\right] \,,\end{aligned} \tag{D.1a}$$

$$J_{20}\,(t,u) = \log\left(\frac{M_\gamma(m_\tau^2 - t)}{m_\tau\, x_+(t,u)}\right) \ , \tag{D.1b}$$

$$J_{02}\,(t,u) = \log\left(\frac{M_\gamma(m_\tau^2 + m_0^2 - t - u)}{m_-\, x_+(t,u)}\right) \ , \tag{D.1c}$$

$$K_{20}\,(t,u) = K_{0,2}\,(t,u) = \log\left(\frac{x_-(t,u)}{x_+(t,u)}\right) \ , \tag{D.1d}$$

where

$$\begin{aligned} x_\pm\,(t,u) =& \frac{-m_-^4 + (m_0^2 - t)(m_\tau^2 - u) + m_-^2(m_\tau^2 + m_0^2 + t + u)}{2m_-^2} \\ & \pm \frac{\lambda^{1/2}\,(u, m_\tau^2, m_-^2)\,\lambda^{1/2}\,(t, m_-^2, m_0^2)}{2m_-^2} \ . \end{aligned} \tag{D.2}$$

These expressions are written in terms of

$$Y_{1,2} = \frac{1 - 2\bar{\alpha} \pm \sqrt{(1-2\bar{\alpha})^2 - (1-\bar{\beta}^2)}}{1+\bar{\beta}} \ , \tag{D.3}$$

with

$$\begin{aligned} \bar{\alpha} =& \frac{(m_\tau^2 - t)(m_\tau^2 + m_0^2 - t - u)}{(m_-^2 + m_\tau^2 - u)} \cdot \frac{\lambda(u, m_-^2, m_\tau^2)}{2\bar{\delta}} \ , \\ \bar{\beta} =& -\frac{\sqrt{\lambda(u, m_-^2, m_\tau^2)}}{m_-^2 + m_\tau^2 - u} \ , \\ \bar{\gamma} =& \frac{\sqrt{\lambda(u, m_-^2, m_\tau^2)}}{2\sqrt{\bar{\delta}}} \ , \\ \bar{\delta} =& -m_0^4 m_\tau^2 + m_-^2(m_\tau^2 - t)(m_0^2 - u) - tu(-m_\tau^2 + t + u) \\ & + m_0^2(-m_\tau^4 + tu + m_\tau^2 t + m_\tau^2 u) \ . \end{aligned}$$

Acknowledgments

The work of R. E. has been supported by the European Union's Horizon 2020 Research and Innovation Programme under grant 824093 (H2020-INFRAIA- 2018-1), the Ministerio de Ciencia e Innovación under grant PID2020-112965GB-I00, and by the Secretaria d'Universitats i Recerca del Departament d'Empresa i Coneixement de la Generalitat de Catalunya under grant 2021 SGR 00649. IFAE is partially funded by the CERCA program of the Generalitat de Catalunya. J. A. M. is also supported by MICINN with funding from European Union NextGenerationEU (PRTR-C17.I1) and by Generalitat de Catalunya, and acknowledges Conacyt for his PhD scholarship. P. R. was partly funded by Conacyt's project within 'Paradigmas y Controversias de la Ciencia 2022', number 319395, and by Cátedra Marcos Moshinsky (Fundación Marcos Moshinsky) 2020.

References

[1] M. Davier, A. Hocker and Z. Zhang, *The Physics of Hadronic Tau Decays*, *Rev. Mod. Phys.* **78** (2006) 1043 [hep-ph/0507078].

[2] A. Pich, *Precision Tau Physics*, *Prog. Part. Nucl. Phys.* **75** (2014) 41 [1310.7922].

[3] Flavour Lattice Averaging Group (FLAG) collaboration, *FLAG Review 2021*, *Eur. Phys. J. C* **82** (2022) 869 [2111.09849].

[4] A. Pich and J. Portoles, *The Vector form-factor of the pion from unitarity and analyticity: A Model independent approach*, *Phys. Rev. D* **63** (2001) 093005 [hep-ph/0101194].

[5] D. Gómez Dumm and P. Roig, *Dispersive representation of the pion vector form factor in $\tau \to \pi\pi\nu_\tau$ decays*, *Eur. Phys. J. C* **73** (2013) 2528 [1301.6973].

[6] S. Gonzàlez-Solís and P. Roig, *A dispersive analysis of the pion vector form factor and $\tau^- \to K^- K_S \nu_\tau$ decay*, *Eur. Phys. J. C* **79** (2019) 436 [1902.02273].

[7] M. Jamin, J.A. Oller and A. Pich, *Strangeness changing scalar form-factors*, *Nucl. Phys. B* **622** (2002) 279 [hep-ph/0110193].

[8] B. Moussallam, *Analyticity constraints on the strangeness changing vector current and applications to $\tau \to K\pi\nu_\tau$, $\tau \to K\pi\pi\nu_\tau$*, *Eur. Phys. J. C* **53** (2008) 401 [0710.0548].

[9] D.R. Boito, R. Escribano and M. Jamin, *$K\pi$ vector form-factor, dispersive constraints and $\tau \to \nu_\tau K\pi$ decays*, *Eur. Phys. J. C* **59** (2009) 821 [0807.4883].

[10] D.R. Boito, R. Escribano and M. Jamin, *$K\,\pi$ vector form factor constrained by $\tau \to K\pi\nu_\tau$ and K_{l3} decays*, *JHEP* **09** (2010) 031 [1007.1858].

[11] M. Antonelli, V. Cirigliano, A. Lusiani and E. Passemar, *Predicting the τ strange branching ratios and implications for V_{us}*, *JHEP* **10** (2013) 070 [1304.8134].

[12] V. Bernard, *First determination of $f_+(0)|V_{us}|$ from a combined analysis of $\tau \to K\pi\nu_\tau$ decay and πK scattering with constraints from $K_{\ell 3}$ decays*, *JHEP* **06** (2014) 082 [1311.2569].

[13] R. Escribano, S. Gonzalez-Solis and P. Roig, *$\tau^- \to K^-\eta^{(\prime)}\nu_\tau$ decays in Chiral Perturbation Theory with Resonances*, *JHEP* **10** (2013) 039 [1307.7908].

[14] R. Escribano, S. González-Solís, M. Jamin and P. Roig, *Combined analysis of the decays $\tau^- \to K_S\pi^-\nu_\tau$ and $\tau^- \to K^-\eta\nu_\tau$*, *JHEP* **09** (2014) 042 [1407.6590].

[15] S. Descotes-Genon and B. Moussallam, *Analyticity of $\eta\pi$ isospin-violating form factors and the $\tau \to \eta\pi\nu$ second-class decay*, *Eur. Phys. J. C* **74** (2014) 2946 [1404.0251].

[16] R. Escribano, S. Gonzalez-Solis and P. Roig, *Predictions on the second-class current decays $\tau^- \to \pi^-\eta^{(\prime)}\nu_\tau$*, *Phys. Rev. D* **94** (2016) 034008 [1601.03989].

[17] OPAL collaboration, *A Study of one prong tau decays with a charged kaon*, *Eur. Phys. J. C* **19** (2001) 653 [hep-ex/0009017].

[18] ALEPH collaboration, *Branching ratios and spectral functions of tau decays: Final ALEPH measurements and physics implications*, *Phys. Rept.* **421** (2005) 191 [hep-ex/0506072].

[19] BaBar collaboration, *Measurements of Charged Current Lepton Universality and $|V_{us}|$ using Tau Lepton Decays to $e^-\bar{\nu}_e\nu_\tau$, $\mu^-\bar{\nu}_\mu\nu_\tau$, $\pi^-\nu_\tau$, and $K^-\nu_\tau$*, Phys. Rev. Lett. **105** (2010) 051602 [0912.0242].

[20] OPAL collaboration, *Measurement of the strong coupling constant α_s and the vector and axial vector spectral functions in hadronic tau decays*, Eur. Phys. J. C **7** (1999) 571 [hep-ex/9808019].

[21] CLEO collaboration, *Hadronic structure in the decay $\tau^- \to \pi^-\pi^0\nu_\tau$*, Phys. Rev. D **61** (2000) 112002 [hep-ex/9910046].

[22] Belle collaboration, *High-Statistics Study of the $\tau^- \to \pi^-\pi^0\nu_\tau$ Decay*, Phys. Rev. D **78** (2008) 072006 [0805.3773].

[23] BaBar collaboration, *Measurement of the spectral function for the $\tau^- \to K^-K_S\nu_\tau$ decay*, Phys. Rev. D **98** (2018) 032010 [1806.10280].

[24] Belle collaboration, *Observation of $\tau^- \to \pi^-\nu_\tau e^+e^-$ and search for $\tau^- \to \pi^-\nu_\tau\mu^+\mu^-$*, Phys. Rev. D **100** (2019) 071101 [1908.09353].

[25] D. Gomez Dumm, A. Pich and J. Portoles, *$\tau \to \pi\pi\pi\nu_\tau$ decays in the resonance effective theory*, Phys. Rev. D **69** (2004) 073002 [hep-ph/0312183].

[26] D.G. Dumm, P. Roig, A. Pich and J. Portoles, *$\tau \to \pi\pi\pi\nu_\tau$ decays and the a(1)(1260) off-shell width revisited*, Phys. Lett. B **685** (2010) 158 [0911.4436].

[27] D.G. Dumm, P. Roig, A. Pich and J. Portoles, *Hadron structure in $\tau \to KK\pi\nu_\tau$ decays*, Phys. Rev. D **81** (2010) 034031 [0911.2640].

[28] D. Gomez Dumm and P. Roig, *Resonance Chiral Lagrangian analysis of $\tau^- \to \eta^{(\prime)}\pi^-\pi^0\nu_\tau$ decays*, Phys. Rev. D **86** (2012) 076009 [1208.1212].

[29] O. Shekhovtsova, T. Przedzinski, P. Roig and Z. Was, *Resonance chiral Lagrangian currents and τ decay Monte Carlo*, Phys. Rev. D **86** (2012) 113008 [1203.3955].

[30] I.M. Nugent, T. Przedzinski, P. Roig, O. Shekhovtsova and Z. Was, *Resonance chiral Lagrangian currents and experimental data for $\tau^- \to \pi^-\pi^-\pi^+\nu_\tau$*, Phys. Rev. D **88** (2013) 093012 [1310.1053].

[31] J.J. Sanz-Cillero and O. Shekhovtsova, *Refining the scalar and tensor contributions in $\tau \to \pi\pi\pi\nu_\tau$ decays*, JHEP **12** (2017) 080 [1707.01137].

[32] JPAC collaboration, *Pole position of the $a_1(1260)$ from τ-decay*, Phys. Rev. D **98** (2018) 096021 [1810.00016].

[33] S. Arteaga, L.-Y. Dai, A. Guevara and P. Roig, *Tension between $e^+e^- \to \eta\pi^-\pi^+$ and $\tau^- \to \eta\pi^-\pi^0\nu_\tau$ data and nonstandard interactions*, Phys. Rev. D **106** (2022) 096016 [2209.15537].

[34] E.A. Garcés, M. Hernández Villanueva, G. López Castro and P. Roig, *Effective-field theory analysis of the $\tau^- \to \eta^{(\prime)}\pi^-\nu_\tau$ decays*, JHEP **12** (2017) 027 [1708.07802].

[35] V. Cirigliano, A. Crivellin and M. Hoferichter, *No-go theorem for nonstandard explanations of the $\tau \to K_S\pi\nu_\tau$ CP asymmetry*, Phys. Rev. Lett. **120** (2018) 141803 [1712.06595].

[36] J.A. Miranda and P. Roig, *Effective-field theory analysis of the $\tau^- \to \pi^-\pi^0\nu_\tau$ decays*, JHEP **11** (2018) 038 [1806.09547].

[37] V. Cirigliano, A. Falkowski, M. González-Alonso and A. Rodríguez-Sánchez, *Hadronic τ Decays as New Physics Probes in the LHC Era*, *Phys. Rev. Lett.* **122** (2019) 221801 [1809.01161].

[38] J. Rendón, P. Roig and G. Toledo Sánchez, *Effective-field theory analysis of the $\tau^- \to (K\pi)^- \nu_\tau$ decays*, *Phys. Rev. D* **99** (2019) 093005 [1902.08143].

[39] F.-Z. Chen, X.-Q. Li, Y.-D. Yang and X. Zhang, *CP asymmetry in $\tau \to K_S \pi \nu_\tau$ decays within the Standard Model and beyond*, *Phys. Rev. D* **100** (2019) 113006 [1909.05543].

[40] S. Gonzàlez-Solís, A. Miranda, J. Rendón and P. Roig, *Effective-field theory analysis of the $\tau^- \to K^-(\eta^{(\prime)}, K^0)\nu_\tau$ decays*, *Phys. Rev. D* **101** (2020) 034010 [1911.08341].

[41] S. Gonzàlez-Solís, A. Miranda, J. Rendón and P. Roig, *Exclusive hadronic tau decays as probes of non-SM interactions*, *Phys. Lett. B* **804** (2020) 135371 [1912.08725].

[42] F.-Z. Chen, X.-Q. Li and Y.-D. Yang, *CP asymmetry in the angular distribution of $\tau \to K_S \pi \nu_\tau$ decays*, *JHEP* **05** (2020) 151 [2003.05735].

[43] M.A. Arroyo-Ureña, G. Hernández-Tomé, G. López-Castro, P. Roig and I. Rosell, *One-loop determination of $\tau \to \pi(K)\nu_\tau[\gamma]$ branching ratios and new physics tests*, *JHEP* **02** (2022) 173 [2112.01859].

[44] M.A. Arroyo-Ureña, G. Hernández-Tomé, G. López-Castro, P. Roig and I. Rosell, *Radiative corrections to $\tau \to \pi(K)\nu_\tau[\gamma]$: A reliable new physics test*, *Phys. Rev. D* **104** (2021) L091502 [2107.04603].

[45] F.-Z. Chen, X.-Q. Li, S.-C. Peng, Y.-D. Yang and H.-H. Zhang, *CP asymmetry in the angular distributions of $\tau \to K_S \pi \nu_\tau$ decays. Part II. General effective field theory analysis*, *JHEP* **01** (2022) 108 [2107.12310].

[46] V. Cirigliano, D. Díaz-Calderón, A. Falkowski, M. González-Alonso and A. Rodríguez-Sánchez, *Semileptonic tau decays beyond the Standard Model*, *JHEP* **04** (2022) 152 [2112.02087].

[47] Z.-H. Guo and P. Roig, *One meson radiative tau decays*, *Phys. Rev. D* **82** (2010) 113016 [1009.2542].

[48] A. Guevara, G. López Castro and P. Roig, *Weak radiative pion vertex in $\tau^- \to \pi^- \nu_\tau \ell^+ \ell^-$ decays*, *Phys. Rev. D* **88** (2013) 033007 [1306.1732].

[49] A. Guevara, G.L. Castro and P. Roig, *Improved description of dilepton production in $\tau^- \to \nu_\tau P^-$ decays*, *Phys. Rev. D* **105** (2022) 076007 [2111.09994].

[50] V. Cirigliano, G. Ecker and H. Neufeld, *Isospin violation and the magnetic moment of the muon*, *Phys. Lett.* **B513** (2001) 361 [hep-ph/0104267].

[51] V. Cirigliano, G. Ecker and H. Neufeld, *Radiative tau decay and the magnetic moment of the muon*, *JHEP* **08** (2002) 002 [hep-ph/0207310].

[52] F. Flores-Baez, A. Flores-Tlalpa, G. Lopez Castro and G. Toledo Sanchez, *Long-distance radiative corrections to the di-pion tau lepton decay*, *Phys. Rev. D* **74** (2006) 071301 [hep-ph/0608084].

[53] J.A. Miranda and P. Roig, *New τ-based evaluation of the hadronic contribution to the vacuum polarization piece of the muon anomalous magnetic moment*, *Phys. Rev. D* **102** (2020) 114017 [2007.11019].

[54] J.L. Gutiérrez Santiago, G. López Castro and P. Roig, *Lepton-pair production in dipion τ lepton decays*, Phys. Rev. D **103** (2021) 014027 [2012.01587].

[55] C. Chen, C.-G. Duan and Z.-H. Guo, *Triple-product asymmetry in the radiative two-pion tau decay*, JHEP **08** (2022) 144 [2201.12764].

[56] F.V. Flores-Baéz and J.R. Morones-Ibarra, *Model Independent Electromagnetic corrections in hadronic τ decays*, Phys. Rev. D **88** (2013) 073009 [1307.1912].

[57] A. Guevara, G. López-Castro and P. Roig, *$\tau^- \to \eta^{(\prime)}\pi^-\nu_\tau\gamma$ decays as backgrounds in the search for second class currents*, Phys. Rev. **D95** (2017) 054015 [1612.03291].

[58] F.E. Low, *Bremsstrahlung of very low-energy quanta in elementary particle collisions*, Phys. Rev. **110** (1958) 974.

[59] A. Sirlin, *Radiative corrections to G_V/G_μ in simple extensions of the $SU(2) \times U(1)$ gauge model*, Nucl. Phys. B **71** (1974) 29.

[60] A. Sirlin, *Current Algebra Formulation of Radiative Corrections in Gauge Theories and the Universality of the Weak Interactions*, Rev. Mod. Phys. **50** (1978) 573.

[61] A. Sirlin, *Large m_W, m_Z Behavior of the $O(\alpha)$ Corrections to Semileptonic Processes Mediated by W*, Nucl. Phys. B **196** (1982) 83.

[62] W.J. Marciano and A. Sirlin, *Radiative Corrections to beta Decay and the Possibility of a Fourth Generation*, Phys. Rev. Lett. **56** (1986) 22.

[63] W.J. Marciano and A. Sirlin, *Electroweak Radiative Corrections to tau Decay*, Phys. Rev. Lett. **61** (1988) 1815.

[64] W.J. Marciano and A. Sirlin, *Radiative corrections to $\pi_{\ell 2}$ decays*, Phys. Rev. Lett. **71** (1993) 3629.

[65] E. Braaten and C.-S. Li, *Electroweak radiative corrections to the semihadronic decay rate of the tau lepton*, Phys. Rev. D **42** (1990) 3888.

[66] J. Erler, *Electroweak radiative corrections to semileptonic tau decays*, *Rev. Mex. Fis.* **50** (2004) 200 [hep-ph/0211345].

[67] T.H. Burnett and N.M. Kroll, *Extension of the low soft photon theorem*, Phys. Rev. Lett. **20** (1968) 86.

[68] V. Cirigliano, M. Giannotti and H. Neufeld, *Electromagnetic effects in $K_{\ell 3}$ decays*, JHEP **11** (2008) 006 [0807.4507].

[69] D. Gomez Dumm, A. Pich and J. Portoles, *The Hadronic off-shell width of meson resonances*, Phys. Rev. D **62** (2000) 054014 [hep-ph/0003320].

[70] G. Ecker, J. Gasser, A. Pich and E. de Rafael, *The Role of Resonances in Chiral Perturbation Theory*, Nucl. Phys. **B321** (1989) 311.

[71] J. Wess and B. Zumino, *Consequences of anomalous Ward identities*, Phys. Lett. **37B** (1971) 95.

[72] E. Witten, *Global Aspects of Current Algebra*, Nucl. Phys. **B223** (1983) 422.

[73] J. Bijnens, G. Ecker and J. Gasser, *Radiative semileptonic kaon decays*, Nucl. Phys. **B396** (1993) 81 [hep-ph/9209261].

[74] K. Kampf and J. Novotny, *Resonance saturation in the odd-intrinsic parity sector of low-energy QCD*, Phys. Rev. **D84** (2011) 014036 [1104.3137].

[75] G. Ecker, J. Gasser, H. Leutwyler, A. Pich and E. de Rafael, *Chiral Lagrangians for Massive Spin 1 Fields*, *Phys. Lett.* **B223** (1989) 425.

[76] V. Cirigliano, G. Ecker, M. Eidemuller, A. Pich and J. Portoles, *The $\langle VAP \rangle$ Green function in the resonance region*, *Phys. Lett. B* **596** (2004) 96 [hep-ph/0404004].

[77] V. Cirigliano, G. Ecker, M. Eidemuller, R. Kaiser, A. Pich and J. Portoles, *Towards a consistent estimate of the chiral low-energy constants*, *Nucl. Phys.* **B753** (2006) 139 [hep-ph/0603205].

[78] P. Roig and J.J. Sanz Cillero, *Consistent high-energy constraints in the anomalous QCD sector*, *Phys. Lett. B* **733** (2014) 158 [1312.6206].

[79] P. Roig and P. Sanchez-Puertas, *Axial-vector exchange contribution to the hadronic light-by-light piece of the muon anomalous magnetic moment*, *Phys. Rev. D* **101** (2020) 074019 [1910.02881].

[80] Z.-H. Guo and J.A. Oller, *Resonances from meson-meson scattering in U(3) CHPT*, *Phys. Rev. D* **84** (2011) 034005 [1104.2849].

[81] Z.-H. Guo, J.A. Oller and J. Ruiz de Elvira, *Chiral dynamics in form factors, spectral-function sum rules, meson-meson scattering and semi-local duality*, *Phys. Rev. D* **86** (2012) 054006 [1206.4163].

[82] Z.-H. Guo, L. Liu, U.-G. Meißner, J.A. Oller and A. Rusetsky, *Chiral study of the $a_0(980)$ resonance and $\pi\eta$ scattering phase shifts in light of a recent lattice simulation*, *Phys. Rev. D* **95** (2017) 054004 [1609.08096].

[83] V. Cirigliano, M. Knecht, H. Neufeld, H. Rupertsberger and P. Talavera, *Radiative corrections to $K_{\ell 3}$ decays*, *Eur. Phys. J. C* **23** (2002) 121 [hep-ph/0110153].

[84] HFLAV collaboration, *Averages of b-hadron, c-hadron, and τ-lepton properties as of 2021*, 2206.07501.

[85] V. Cirigliano, H. Neufeld and H. Pichl, *K_{e3} decays and CKM unitarity*, *Eur. Phys. J. C* **35** (2004) 53 [hep-ph/0401173].

[86] S. Weinberg, *Phenomenological Lagrangians*, *Physica A* **96** (1979) 327.

[87] J. Gasser and H. Leutwyler, *Chiral Perturbation Theory to One Loop*, *Annals Phys.* **158** (1984) 142.

[88] J. Gasser and H. Leutwyler, *Chiral Perturbation Theory: Expansions in the Mass of the Strange Quark*, *Nucl. Phys. B* **250** (1985) 465.

[89] A. Flores-Tlalpa, *Modelo de dominancia de mesones para decaimientos semileptónicos de sabores pesados*, Ph.D. thesis, CINVESTAV, IPN, 2008.